Czech Technical University in Prague

Faculty of Electrical Engineering

Department of Electrical power Engineering

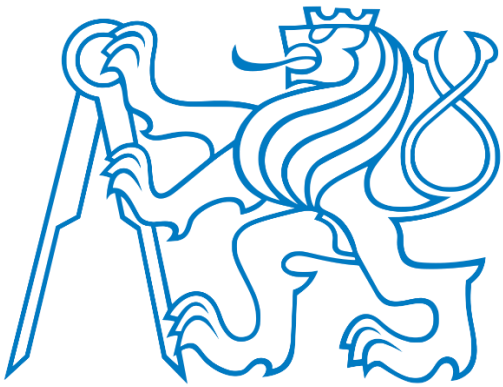

Diploma Thesis

Low-carbon technology in distribution networks
Nizkokarbonové technologie v distribuönich sitich

Author: Abdullah Essa

Supervisor: Ing. Josef Hrouda

CTU CZECH TECHNICAL UNIVERSITY IN PRAGUE

MASTER'S THESIS ASSIGNMENT

I. Personal and study details

Student's name: **Essa Abdullah** Personal ID number: **453523**

Faculty / Institute: **Faculty of Electrical Engineering**

Department / Institute: **Department of Electrical Power Engineering**

Study program: **Electrical Engineering, Power Engineering and Management**

Specialisation: **Electrical Power Engineering**

II. Master's thesis details

Master's thesis title in English:

Low-carbon technology in distribution networks

Master's thesis title in Czech:

Nízkokarbonové technologie v distribučních sítích

Guidelines:

-A general description of renewables, with a focus on solar systems: Isolated, stand-alone, and connected to grid types.
-Flexibility of consumption and production
-Description of micro-grids and mentioning examples that exist in real life.
-Case study

Bibliography / sources:

[1]https://www.ise.fraunhofer.de/content/dam/ise/de/documents/publications/studies/Photovoltaics-Report.pdf
accessed on the 4th of May 2018.
[2]https://www.carbonbrief.org/global-solar-capacity-grew-faster-than-fossil-fuels-2017-report
accessed on the 6th of May 2018.
[3]http://ec.europa.eu/environment/waste/weee/pdf/Study%20on%20PVs%20Bio%20final.pdf
accessed on the 4th of May 2018
[4]https://www.nrel.gov/pv/research.html accessed on the 29th of April 2018

Name and workplace of master's thesis supervisor:

doc. Dr. Ing. Jan Kyncl, Department of Electrical Power Engineering, FEE

Name and workplace of second master's thesis supervisor or consultant:

Date of master's thesis assignment: **24.02.2020** Deadline for master's thesis submission: **22.05.2020**

Assignment valid until: **19.02.2022**

doc. Dr. Ing. Jan Kyncl Supervisor's signature	Head of department's signature	prof. Mgr. Petr Páta, Ph.D. Dean's signature

III. Assignment receipt

The student acknowledges that the master's thesis is an individual work. The student must produce his thesis without the assistance of others, with the exception of provided consultations. Within the master's thesis, the author must state the names of consultants and include a list of references.

Date of assignment receipt Student's signature

Declaration

I hereby declare that this thesis is the result of my own work and all the sources I used are in the list of references, in accordance with Methodological Instructions of Ethical Principle in the Preparation of University Thesis.

In Prague, 22.5.2020

Acknowledgement

First and foremost, I would like to express my deep and sincere gratitude to my supervisor Ing. Josef Hrouda for providing invaluable guidance and support throughout my writing of this thesis. It was a great privilege and honor to work and study under his guidance.

I also would like to thank doc. Ing. Jan Kyncl for his constant support, availability and constructive suggestions, which were determinant for the accomplishment of the work presented in this thesis.

Finally, I must express my very profound gratitude to my parents and to my friends for providing me with unfailing support and continuous encouragement throughout my years of study and through the process of researching and writing this thesis. This accomplishment would not have been possible without them.

Nizkokarbonové technologie v distribuönich sitich

Abstrakt

Abnovitelné zdroje energie (OZE) v distribučních soustavách (DS) nabývají na důležtitosti a v budoucnu budou hrát v DS důležitou roli. Tato diplomová práce popisuje základní informace o OZE a jejich principech činnosti. V práci je shrnuto současné i budoucí využití OZE v různých částech světa. V práci jsou také uvedena legislativní pravidla pro připojování OZE k DS. Na případové studii je ověřena připojitelnost 2 MW větrné elektrárny k DS z pohledu vyvolané napěťové změny a flikru.

Klíčová slova:

Obnovitelné zdroje energie, výrobna elektřiny, vodní elektrárna, fotovoltaická elektrárna, větrná elektrárna, distribuční soustava, DNCalc software, ustálený chod, studie připojitelnosti, flikr

Low-carbon technology in distribution networks

Abstract

Renewable energy sources (RES) are gaining an increasing importance in the distribution system and they are predicted to play a more important role in the near future. This thesis will provide general information about renewable energy sources and their working principles. The present and future usage of RES is summarized for different regions in the world. Legislation and rules about connecting into the distribution grid has been presented. Besides, a case study demonstrates the evaluation of connectivity of a 2 MW wind power plant to a distribution network from the perspective of voltage change and flicker effect.

Keywords:

Renewable energy sources, Power generation, Hydropower energy, Solar energy, Wind energy, Power plants, Distribution System, DNCalc software, Load Flow, Study of connectivity, Flicker

Table of Contents

List of Abbreviations

EU	European Union
GHG	Greenhouse Gases
RES	Renewable Energy Sources
OCGT	Open Cycle Gas Turbine
CCGT	Combined Cycle Gas Turbines
CO2	Carbon Dioxide
IRENA	International Renewable Energy Agency
PV	Photovoltaic
NREA	New and Renewable Energy Authority
DFIG	Doubly Fed Induction Generator
WECS	Wind Energy Conversion Systems
WT	Wind Turbine
PEC	Power Electronic Converter
RSC	Rotor Side Converter
VSC	Voltage Source Converter
IGBT	Insulated Gate Bipolar Transistors
DC	Direct Current
SPWM	Sinusoidal Pulse Width Modulation
SVM	Space Vector Modulation
GSC	Grid Side Converter
EMC	Electromagnetic Compatibility
THD	Total Harmonic Distortion
CCU	Converter Control Unit
VSWT	Variable Speed Wind Turbine
MPPT	Maximum Power Point Tracking
HV	High Voltage
MV	Medium Voltage
LV	Low Voltage
WPP	Wind Power PLant
DTS	Distribution Transformer Stations
PCC	Point of Common Coupling

List of Figures

1 Introduction

There is an increasing need for energy and its associated services to satisfy human social and economic development, welfare, and health. Securing energy supply and curbing energy contribution to climate change, however, are the energy sector's two-over-riding threats on the road to a sustainable future.

Dominance of fossil-fuel - based power generation (Coal , Oil and Gas) and exponential population growth over the past decades have led to growing energy demand resulting in global problems associated with rapid growth in carbon dioxide (CO2) emissions. A severe climate change has been one of the twenty-first century's greatest threats. Its serious impacts could still be stopped if attempts are taken to change current energy systems.

Renewable energy sources hold the key potential to displace greenhouse gas emissions from fossil fuel-based power generating and thereby mitigating climate change. Since renewable energy supplies are derived naturally from the ongoing flows of energy in our surroundings, it should be sustainable. Renewable energy sources replenish themselves naturally without being depleted in the earth; they include bioenergy, hydropower, geothermal energy, solar energy, wind energy and ocean (tide and wave) energy.

Despite the outstanding benefits of renewable energy sources, there are certain shortcomings, such as: the discontinuity of generation due to seasonal variations as most renewable energy resources are climate-dependent, which is why its exploitation requires complex methods of design , planning and optimization control. Fortunately, the continuous technological advances in computer hardware and software are permitting scientific researchers to handle these optimization difficulties using computational resources applicable to the renewable and sustainable energy field.

2 Overview of renewable sources

Renewable energy sources are energy sources from natural and persistent flow of energy happening in our immediate environment. They include: hydropower, solar energy, and wind energy.

2.1 Hydropower

Hydroelectric power, electricity produced from turbine-driven generators which converts the potential energy of falling or fast-flowing water into mechanical energy. In order to generate electricity from the kinetic energy in moving water, the water has to move with sufficient speed and volume to spin a propeller-like mechanism called a turbine, which in turn rotates a generator [1].

There are a number of turbine types used in hydropower systems, and their usage depends on the amount of hydraulic head (vertical distance between the dam and the turbine) at the plant. The most common are Kaplan, Francis, and Pelton wheel designs. Some of these designs not only use just the kinetic force of the moving water but also the water pressure.

2.1.1 Components and working principle of a hydropower plant

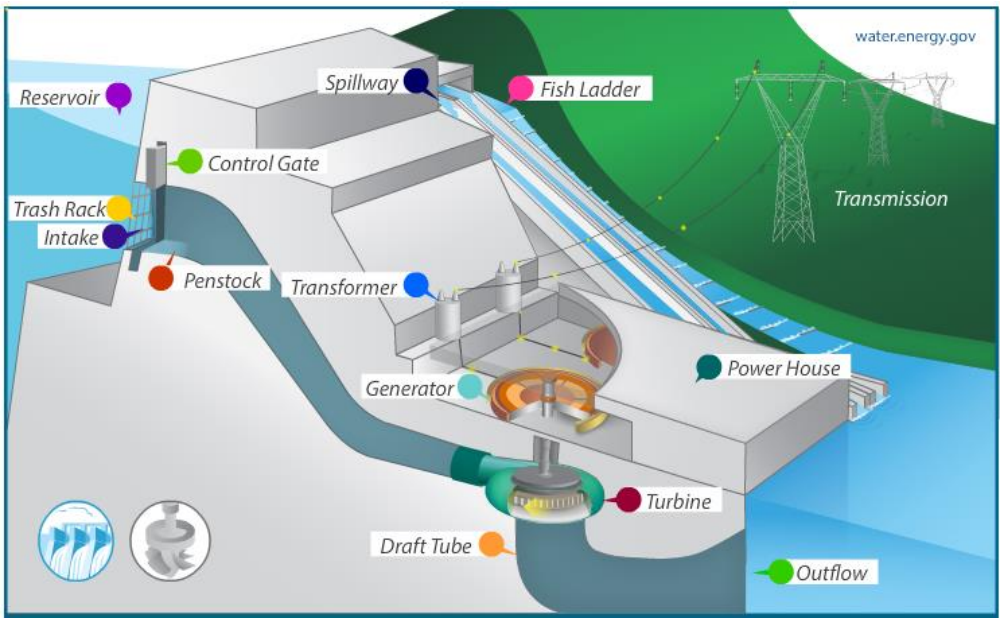

Figure 2.1 - Main components of a hydropower plant [1]

- **Reservoir:** The body of water that builds up behind dams. The stored energy that is contained in the reservoir is converted into kinetic energy once the control gate opens and the water flows through it.
- **Trash Rack:** A screen typically comprised of metal or concrete bars that prevents debris from entering the penstock.

- **Intake:** The section of the reservoir immediately in front of the control gate where water is drawn into the penstock.
- **Penstock:** Water travels into this channel from the intake, forcing it to run through the turbine.
- **Control Gate, Turbine:** As water runs through the blades of the turbine, it forces them to spin, turning a shaft that is connected to the generator. Pictured is Francis, the most common type of hydropower turbine.
- **Spillway:** This structure allows water to be released in a controlled fashion from the dam downstream into the river, controlling flood situations – "a safety valve" for the facility.
- **Fish Ladder:** This structure allows fish to migrate past a dam by providing them a series of steps to swim and leap up to reach the other side of the dam.
- **Transformer:** Here, the electricity produced is converted to a higher voltage to travel into the transmission grid.
- **Generator:** As the turbine runner is moved by water the connected shaft spins the generator producing the electricity. In general we can divide generators into: induction machine based generators (asynchronous) and synchronous generators. In case of using synchronous generators, speed governors and exciters are needed. While in case of using asynchronous generators, reactive power compensation is commonly used (capacitors)
- **Power House:** This section houses the generators, turbines, and the controls.
- **Draft Tube:** After water exits the turbine the draft tube slows down the water to keep the turbine under a more constant pressure, which increases turbine efficiency.
- **Outflow:** The measure of water released from the dam during a certain period.
- **Transmission:** Here, the electricity produced is converted to a higher voltage to travel into the transmission grid.

2.1.2 Components and working principle of a hydropower turbine

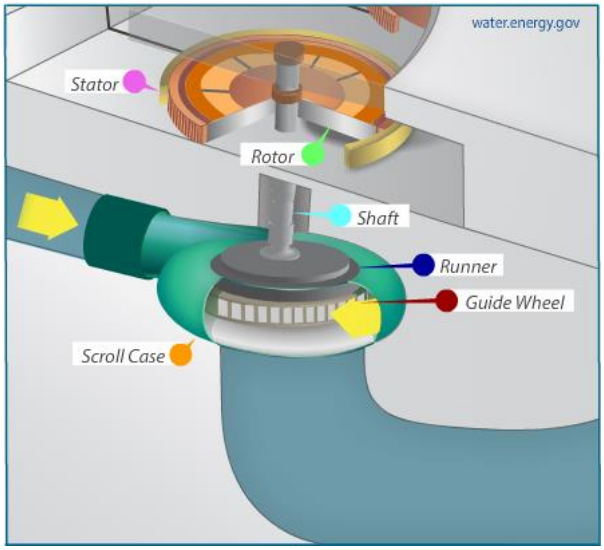

Figure 2.2 – Main components of a hydropower turbine [2]

- **Stator:** Often made of a series of magnets, is the stationary part of a rotary generator system. The water moves the runner, which spins the shaft and the conductive rotor inside the stationary magnetic stator producing an alternating electric current.
- **Rotor:** Often made of copper wire or other conductive material, is the spinning part of a rotary generator system.
- **Shaft:** Connects the turbine with generator.
- **Runner:** The Blades of Turbine are known as the runner, and their shape determines the flow of water and amount of energy extracted.
- **Guide Wheel:** Is used to focus the flow of water directly onto the turbine blades, which are also called the runner.
- **Scroll Case:** Allows water to travel smoothly from the penstock through the turbine.

2.2 Solar Energy

Solar power is usable energy generated from the sun in the form of electric or thermal energy. Solar energy is captured in a variety of ways, the most common of which is with photovoltaic solar panels that convert the sun's rays into usable electricity. Aside from using photovoltaics to generate electricity, solar energy is commonly used in thermal applications to heat indoor spaces or fluids.

Solar energy is a clean, inexpensive, renewable power source that is harnessable nearly everywhere in the world - any point where sunlight hits the surface of the earth is a potential location to generate solar power. And since solar energy comes from the sun, it represents a limitless source of power.

2.2.1 Components and working principle of a photovoltaic cell

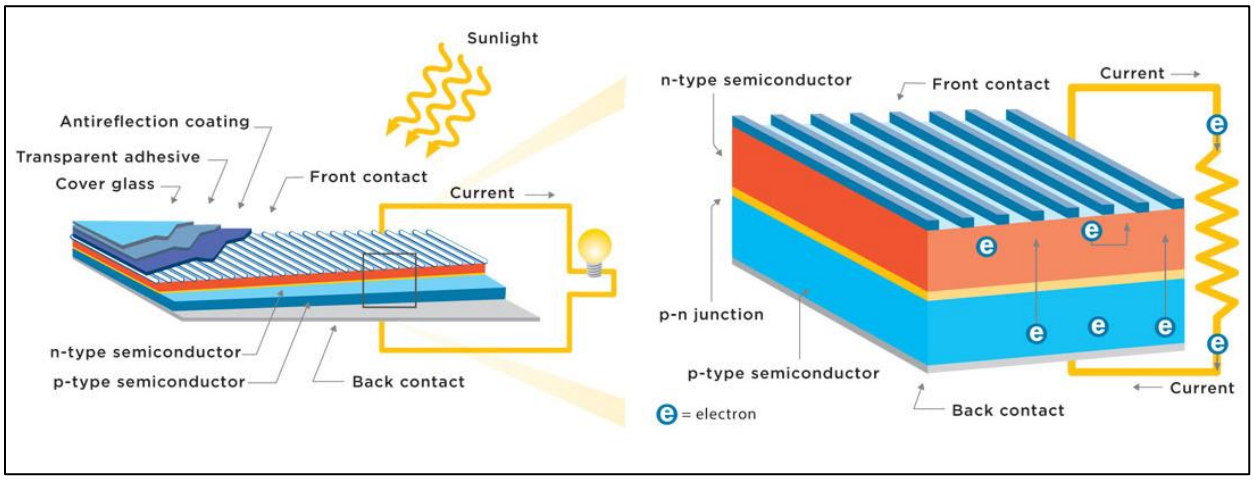

Figure 2.3 – Main components of a photovoltaic cell [3]

Conversion of light energy in electrical energy is based on a phenomenon called photovoltaic effect. When semiconductor materials are exposed to light, the some of the photons of light ray are absorbed by the semiconductor crystal which causes a significant number of free electrons in the crystal. This is the basic reason for producing electricity due to photovoltaic effect. Photovoltaic cell is the basic unit of the system where the photovoltaic effect is utilised to produce electricity from light energy. Silicon is the most widely used semiconductor material for constructing the photovoltaic cell. While light ray strikes on any materials some portion of the light is reflected, some portion is transmitted through the materials and rest is absorbed by the materials. The antireflection coating improves the amount of light absorbed.

The same thing happens when light falls on a silicon crystal. If the intensity of incident light is high enough, sufficient numbers of photons are absorbed by the crystal and these photons, in turn, excite some of the electrons of covalent bonds. These excited electrons then get sufficient energy to migrate from valence band to conduction band. As the energy level of these electrons is in the conduction band, they leave from the covalent bond leaving a hole in the bond behind each removed electron. These are called free electrons and they move randomly inside the crystal structure of the silicon.

These light generated electrons and holes cannot produce electricity in the silicon crystal alone. Some additional mechanisms could do that: Impurities, such as, Phosphorus and Boron. By adding impurities, say Phosphorus, loosely bounded electrons will be availabe. Even at room temperature, the thermal energy available in the crystal is large enough to disassociate these relatively loose electrons from their parent phosphorus atom. While this extra relatively loose electron is disassociated from parent phosphorus atom, the phosphorous atom immobile positive ions. The said disassociated electron becomes free but does not have any incomplete covalent bond or hole in the crystal to be re-associated.

These free electrons come from pentavalent impurity and are always ready to conduct current in the semiconductor.

On the other hand, impurities like Boron when added to the the mix, “holes” are developed. It can be said that holes also can move freely as free electrons inside semiconductor crystal.

In a nutshell, in n-type semiconductor mainly the free electrons carry negative charge and in p-type semiconductor mainly the holes in turn carry positive charge therefore free electrons in n-type semiconductor and free holes in p-type semiconductor are called majority carrier in n-type semiconductor and p-type semiconductor respectively.

There is always a potential barrier between n-type and p-type material. This potential barrier is essential for working of a photovoltaic cell. While n-type semiconductor and p-type semiconductor contact each other, the free electrons near to the contact surface of n-type semiconductor get plenty of adjacent holes of p-type material. Hence free electrons and valence electrons in n-type semiconductor near to its contact surface come out from the covalent bond and recombine with more nearby holes in the p-type semiconductor. As the covalent bonds are broken, there will be a number of holes created in the n-type material near the contact surface. Hence, near contact zone, the holes in the p-type materials disappear due to recombination on the other hand holes appear in the n-type material near same contact zone. This is as such equivalent to the migration of holes from p-type to the n-type semiconductor. So as soon as one n-type semiconductor and one p-type semiconductor come into contact the electrons from n-type will transfer to p-type and holes from p-type will transfer to n-type. The process is very fast but does not continue forever. After some instant, there will be a layer of negative charge (excess electrons) in the p-type semiconductor adjacent to the contact along the contact surface. Similarly, there will be a layer of positive charge (positive ions) in the n-type semiconductor adjacent to contact along the contact surface. The thickness of these negative and positive charge layer increases up to a certain extent, but after that, no more electrons will migrate from n-type semiconductor to p-type semiconductor. This is because, while any electron of n-type semiconductor tries to migrate over p-type semiconductor it faces a sufficiently thick layer of positive ions in n-type semiconductor itself where it will drop without crossing it. Similarly, holes will no more migrate to n-type semiconductor from p-type. The holes when trying to cross the negative layer in p-type semiconductor these will recombine with electrons and no more movement toward n-type region. Due to these positive and negative charged layer, there will be an electric field across the region and this region is called depletion layer.

Now let us come to the silicon crystal. When light ray strikes on the crystal, some portion of the light is absorbed by the crystal, and consequently, some of the valence electrons are excited and come out from the covalent bond resulting free electron-hole pairs.

If light strikes on n-type semiconductor the electrons from such light-generated electron-hole pairs are unable to migrate to the p-region since they are not able to cross the potential barrier due to the repulsion

of an electric field across depletion layer. At the same time, the light-generated holes cross the depletion region due to the attraction of electric field of depletion layer where they recombine with electrons, and then the lack of electrons here is compensated by valence electrons of p-region, and this makes as many numbers of holes in the p-region. As such light generated holes are shifted to the p-region where they are trapped because once they come to the p-region cannot be able to come back to n-type region due to the repulsion of potential barrier.

As the negative charge (light generated electrons) is trapped in one side and positive charge (light generated holes) is trapped in opposite side of a cell, there will be a potential difference between these two sides of the cell. This potential difference is typically 0.5 V. This is how a photovoltaic cells or solar cells produce potential difference. [4]

2.3 Wind Energy

Wind energy describes the process by which wind is used to generate electricity. Wind turbines convert the kinetic energy in the wind into mechanical power. A generator can convert mechanical power into electricity.

Wind is caused by the uneven heating of the atmosphere by the sun, variations in the earth's surface, and rotation of the earth. Mountains, bodies of water, and vegetation all influence wind flow patterns. Wind turbines convert the energy in wind to electricity by rotating propeller-like blades around a rotor. The rotor turns the drive shaft, which turns an electric generator. Three key factors affect the amount of energy a turbine can harness from the wind: wind speed, air density, and swept area.

2.3.1 Components and working principle of a wind turbine

For medium and large wind turbines (WT), the doubly-fed induction generator (DFIG) is currently the dominant technology while permanent-magnet (PM), switched reluctance (SR) and high temperature superconducting (HTS) generators are all extensively researched and developed over the years. The main components of the wind turbines are illustrated in figure 2.4.

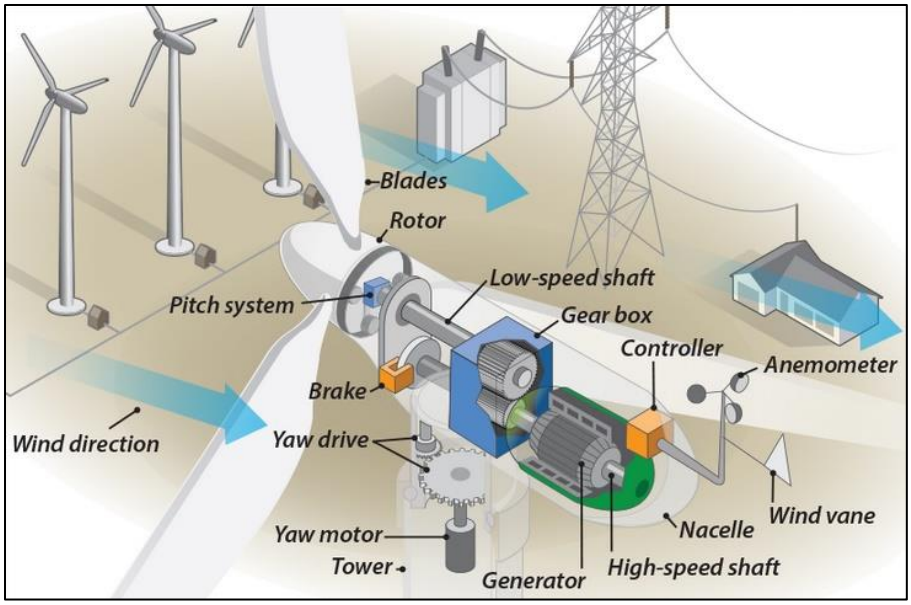

Figure 2.4 – Main components of a wind turbine [5]

- **Wind direction:** Determines the design of the turbine.
- **Tower:** Made from tubular steel, concrete, or steel lattice. Supports the structure of the turbine. Because wind speed increases with height, taller towers enable turbines to capture more energy and generate more electricity.
- **Blades:** Lifts and rotates when wind is blown over them, causing the rotor to spin. Most turbines have either two or three blades.
- **Rotor:** Blades and hub together form the rotor.
- **Pitch system:** Turns blades out of the wind to control the rotor speed, and to keep the rotor from turning in winds that are too high or too low to produce electricity.
- **Brake:** Stops the rotor mechanically, electrically, or hydraulically, in emergencies.
- **Low-speed shaft:** Turns the low-speed shaft at about 30-60 rpm.
- **High-speed shaft:** Drives the generator.
- **Gear box:** Connects the low-speed shaft to the high-speed shaft and increases the rotational speeds from about 30-60 rpm, to about 1000 - 1800 rpm; this is the rotational speed required by most generators to produce electricity. The gear box is a costly and heavy part of the wind turbine. Engineers are exploring "direct-drive" generators that operate at lower rotational speeds and do not need gear boxes.
- **Generator:** Produces 50 - cycle AC electricity; it is usually an off-the-shelf induction generator.
- **Controller:** stars up the machine at wind speeds of about 13 to 26 kilometers per hour (km/h) and shuts off the machine at about 88 km/h. Turbines do not operate at wind speeds above 88 km/h because they may be damaged by the high winds.
- **Anemometer:** Measures the wind speed and transmits wind speed data to the controller.

- **Wind vane:** Measures wind direction and communicates with the yaw drive to orient the turbine properly with respect to the wind.
- **Nacelle:** Sits atop the tower and contains the gear box, low- and high-speed shafts, generator, controller, and brake. Some nacelles are large enough for a helicopter to land on.
- **Yaw motor:** Powers the yaw drive.
- **Yaw drive:** Orients upwind turbines to keep them facing the wind when the direction changes. Downwind turbines don't require a yaw drive because the wind manually blows the rotor away from it.

3 Renewable energy sources (RES) in the European Union (EU)

3.1 Energy production in EU

The energy available in the European Union comes from energy produced in the EU and from energy imported from other countries. The production of energy in the EU is spread across a range of different energy sources: solid fossil fuels, natural gas, crude oil, nuclear energy and renewable energy (such as hydro, wind and solar energy). [6]

Renewable energy (34% of total EU energy production) was the largest contributing source to energy production in the EU in 2018. Nuclear energy (31%) was the second largest source, followed by solid fuels (22%), natural gas (9%) and crude oil (4%) as shown in figure 3.1.

However, the production of energy is very different from one Member State to another. The significance of nuclear energy is particularly high in France (78% of total national energy production), Belgium (65%) and Slovakia (63%). Renewable energy is the main source of energy produced in a number of Member States, with over 90 % (of the energy produced within the country) in Malta, Latvia, Cyprus, Portugal and Lithuania. Solid fuels have the highest importance in Poland (78%), Estonia (74%), Greece (57%) and Czech Republic (55%), while natural gas is the main source of energy produced in the Netherlands (76%). Crude oil is the major source of energy produced in Denmark (41%). [7]

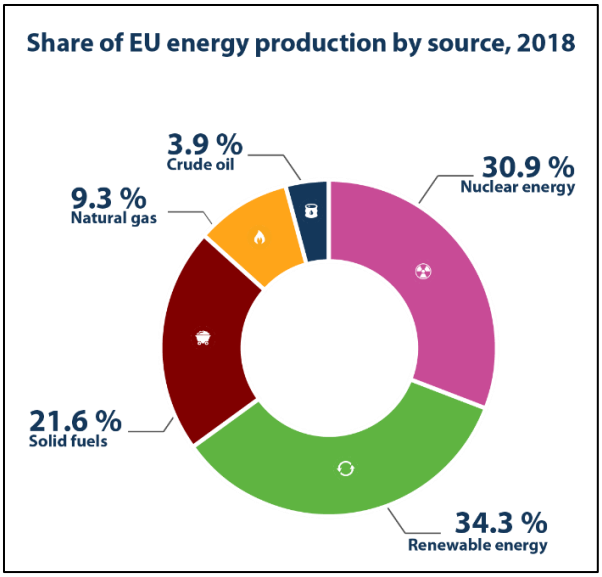

Figure 3.1 - Share of energy production in EU, 2018 [7]

3.2 Emissions of greenhouse gases by the EU

Climate change is a threat to sustainable development. After years of extensive research, the scientific community agrees that man-made greenhouse gas (GHG) emissions are the dominant cause of the Earth's average temperature increases over the past 250 years. Man-made GHG emissions are primarily a by-product of burning of fuels in power plants, cars or homes.

In 2017, EU GHG emissions were down by 19% compared with 1990 levels, representing an absolute reduction of 935 million tonnes of CO2 equivalents, putting the EU on track to meet its 2020 target, which is to reduce GHG emissions by 20% by 2020 and by 40% by 2030 compared with 1990 as shown in figure 3.2.

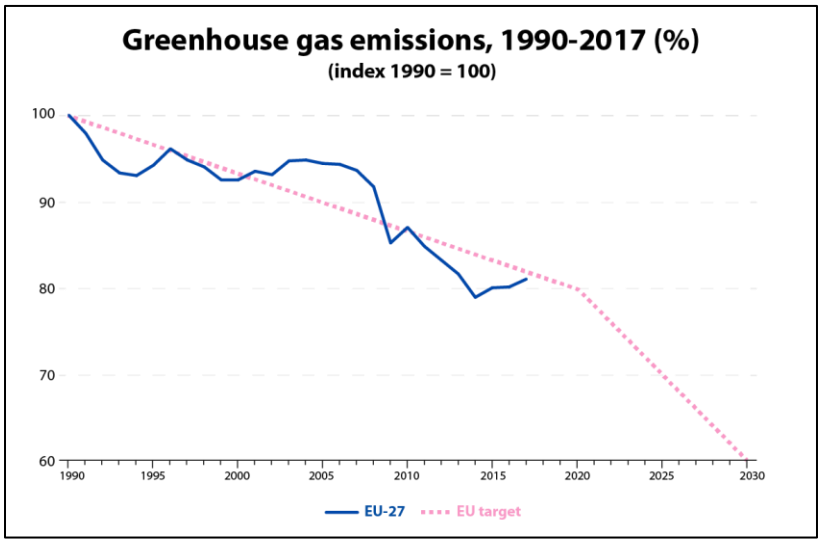

Figure 3.2 – Greenhouse gas emissions in EU, 1990-2017 [7]

3.3 Share of renewable energy in the EU

The share of renewable energy in energy consumption increased continuously between 2004 and 2018, from 9.6% to 18.9%. The Europe 2020 target is 20% by 2020 and the Europe 2030 target is 32% by 2030.

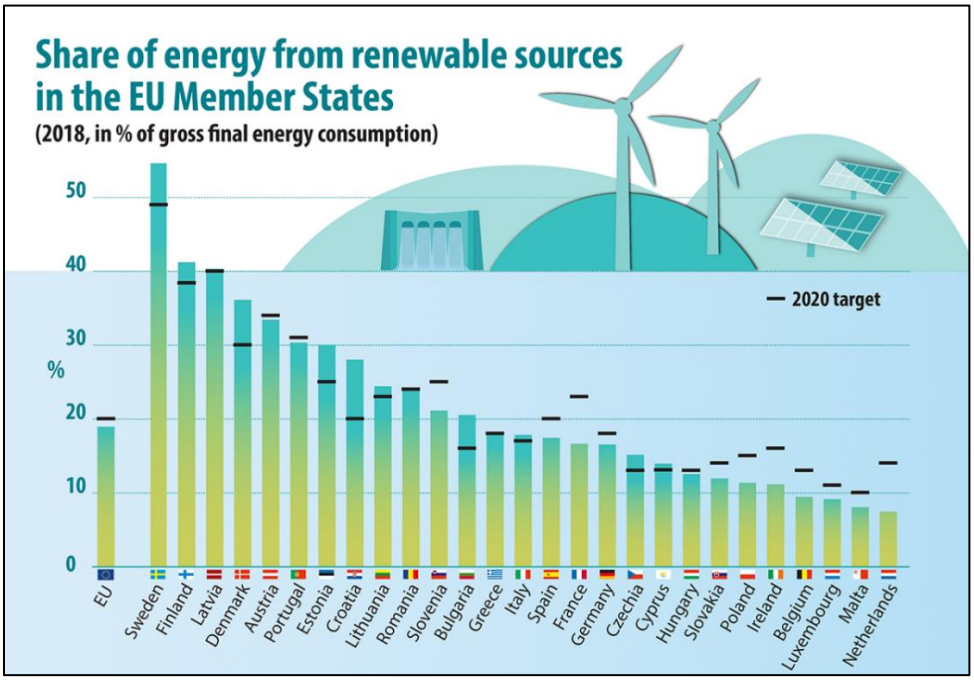

Figure 3.3 – Share of energy from renewable sources in the EU member states [7]

The share of renewable energy in the Member States was highest in Sweden (54.6% of energy consumption) followed by Finland (41.2%) and Latvia (40.3%) as shown in table 3.1. This share was lowest in the Netherlands (7.4%), Malta (8.0%) and Luxembourg (9.1%).

Differences stem from variations in the endowment with natural resources, mostly in the potential for building hydropower plants and in the availability of biomass. All Member States increased their renewable energy share between 2004 and 2018, fourteen have at least doubled their share. [7]

Table 3.1 - Share of energy from renewable sources in EU [7]

Share of energy from renewable sources (in % of gross final energy consumption)						
	2004	**2015**	**2016**	**2017**	**2018**	**2020 target**
EU	8.5	16.7	17.0	17.5	**18.0**	20
Belgium	1.9	8.0	8.7	9.1	**9.4**	13
Bulgaria	9.2	18.3	18.8	18.7	**20.5**	16
Czech Republic	6.8	15.1	14.9	14.8	**15.1**	13
Denmark	14.8	30.9	32.0	35.0	**36.1**	30
Germany	6.2	14.9	14.9	15.5	**16.5**	18
Estonia	18.4	28.2	28.7	29.1	**30.0**	25
Ireland	2.4	9.1	9.3	10.6	**11.1**	16
Greece	7.2	15.7	15.4	17.0	**18.0**	18
Spain	8.3	16.2	17.4	17.6	**17.4**	20
France	9.5	15.0	15.7	16.0	**16.6**	23
Croatia	23.4	29.0	28.3	27.3	**28.0**	20
Italy	6.3	17.5	17.4	18.3	**17.8**	17
Cyprus	3.1	9.9	9.9	10.5	**13.9**	13
Latvia	32.8	37.5	37.1	39.0	**40.3**	40
Lithuania	17.2	25.8	25.6	26.0	**24.4**	23
Luxembourg	0.9	5.0	5.4	6.3	**9.1**	11
Hungary	4.4	14.5	14.3	13.5	**12.5**	13
Malta	0.1	5.1	6.2	7.3	**8.0**	10
Netherlands	2.0	5.7	5.8	6.5	**7.4**	14
Austria	22.6	33.5	33.4	33.1	**33.4**	34
Poland	6.9	11.7	11.3	11.0	**11.3**	15
Portugal	19.2	30.5	30.9	30.6	**30.3**	31
Romania	16.8	24.8	25.0	24.5	**23.9**	24
Slovenia	16.1	21.9	21.3	21.1	**21.1**	25
Slovakia	6.4	12.9	12.0	11.5	**11.9**	14
Finland	29.3	39.3	39.0	40.9	**41.2**	38
Sweden	38.7	53.0	53.4	54.2	**54.6**	49
United Kingdom	0.9	8.3	9.0	9.7	**11.0**	15

Table 3.2 illustrates the total energy production (GWh) from renewable energy sources in all memebers of EU. Germany (179 879 GWh), France (109 758 GWh), and Spain (95 576 GWh) had the highest amount of generation. While, Malta (189.6 GWh), Cyprus (420.5 GWh), and Estonia (681.8 GWh) having the least amount.

Table 3.2 - Renewable energy production (GWh), in 2018 [7]

Country	Hydropower	Wind power	Solar power	Total
Belgium	1,328.8	7,464.7	3,901.8	**12,695.3**
Bulgaria	5,422.7	1,318.1	1,342.8	**8,083.6**
Czech Republic	2,679.4	609.3	2,358.9	**5,647.6**
Denmark	14.9	13,898.8	953.0	**14,866.6**
Germany	24,144.0	109,951.0	45,784.0	**179,879.0**
Estonia	15.0	636.0	30.8	**681.8**
Ireland	931.7	8,639.8	16.7	**9,588.1**
Greece	5,759.9	6,300.3	3,790.7	**15,850.8**
Spain	36,803.0	50,896.0	7,877.0	**95,576.0**
France	70,590.2	28,599.0	10,568.7	**109,758.0**
Croatia	7,784.9	1,335.4	74.9	**9,195.2**
Italy	50,502.8	17,716.4	22,653.8	**90,873.0**
Cyprus	0.0	221.0	199.5	**420.5**
Latvia	2,431.6	122.0	1.3	**2,554.9**
Lithuania	959.6	1,144.0	86.6	**2,190.2**
Luxembourg	1,336.8	254.6	119.7	**1,711.1**
Hungary	222.0	607.0	620.0	**1,449.0**
Malta	0.0	0.1	189.6	**189.6**
Netherlands	72.3	10,563.6	3,693.1	**14,329.1**
Austria	41,215.9	6,030.4	1,437.6	**48,684.0**
Poland	2,387.4	12,798.8	300.5	**15,486.7**
Portugal	13,628.3	12,616.6	1,005.9	**27,250.7**
Romania	18,097.3	6,322.2	1,771.0	**26,190.6**
Slovenia	4,893.0	6.0	255.0	**5,154.0**
Slovakia	3,879.0	6.0	585.0	**4,470.0**
Finland	13,301.1	5,838.7	90.2	**19,230.0**
Sweden	62,250.0	16,623.0	407.0	**79,280.0**
United Kingdom	7,988.2	56,904.0	12,857.4	**77,749.5**

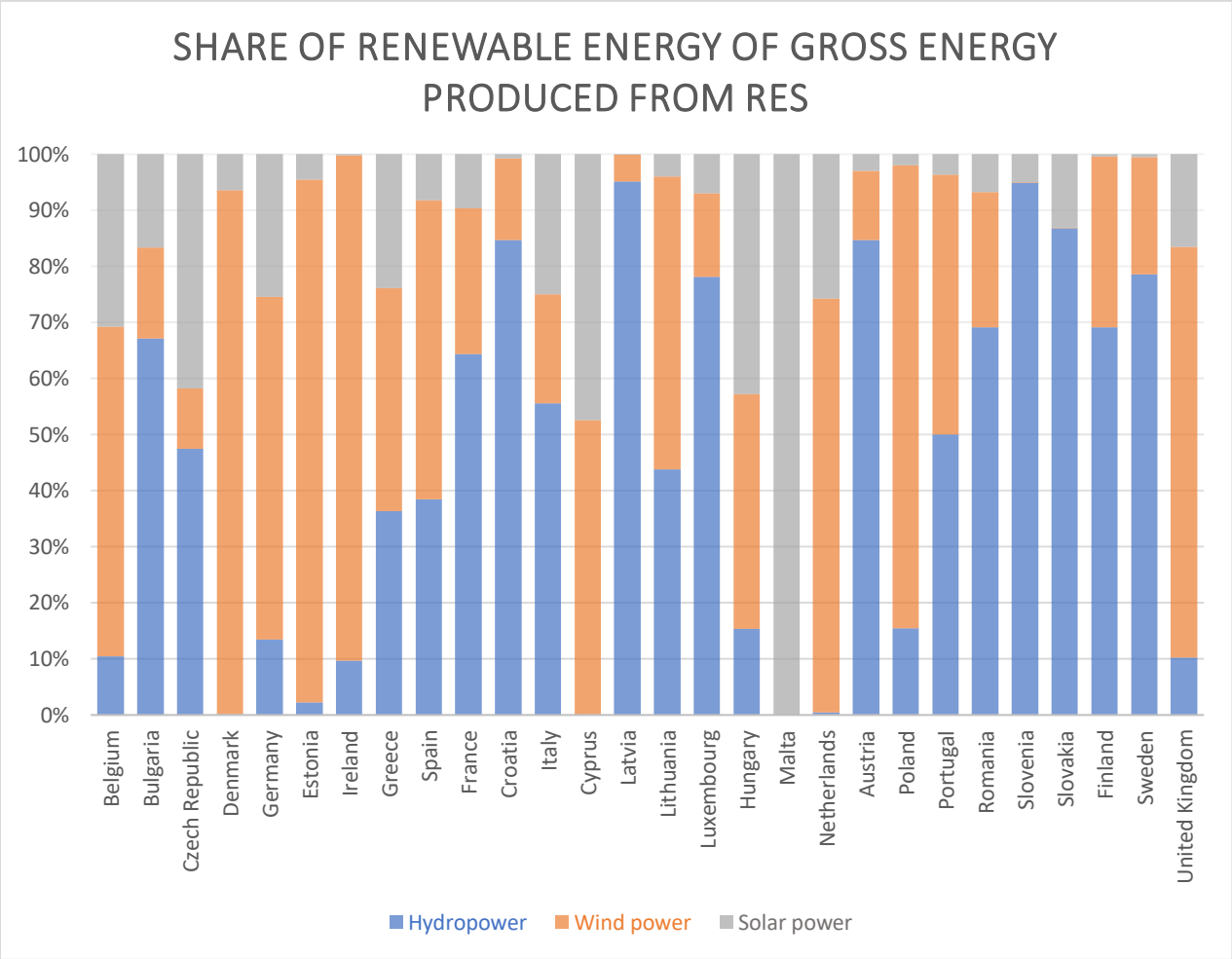

4 Renewable energy sources in Egypt

Egypt, the most populous nation in the Middle East, faces rising energy demand fueled by high population growth and a growing economy. This raises major difficulties in ensuring stable and consistent energy supply. Over the past decade, Egypt's power demand has gradually risen, posting an average growth rate of 6%.

Total installed electricity generation capacity in the year 2015/16 amounted to 38 857 megawatts (MW): comprising open cycle gas turbine (OCGT) power plants (7 845 MW), combined cycle gas turbines (CCGT) power plants (12 527 MW), hydro (2 800 MW), steam power plants (14 798 MW) and non-hydro renewables (887 MW) as highlighted in figure 4.1.

In 2016, the peak load demand was close to installed capacity. Peak load was recorded at 29.2 GW in 2015/16 as highlighted in figure 4.2. Given the increase in installed capacity, total electricity generation in 2015/16 amounted to 186 320 gigawatt hours (GWh), whereas total electricity consumption was 156 300 GWh in 2015/16, resulting in sufficient reserves of over 16.11% to meet electricity demand surges. [8]

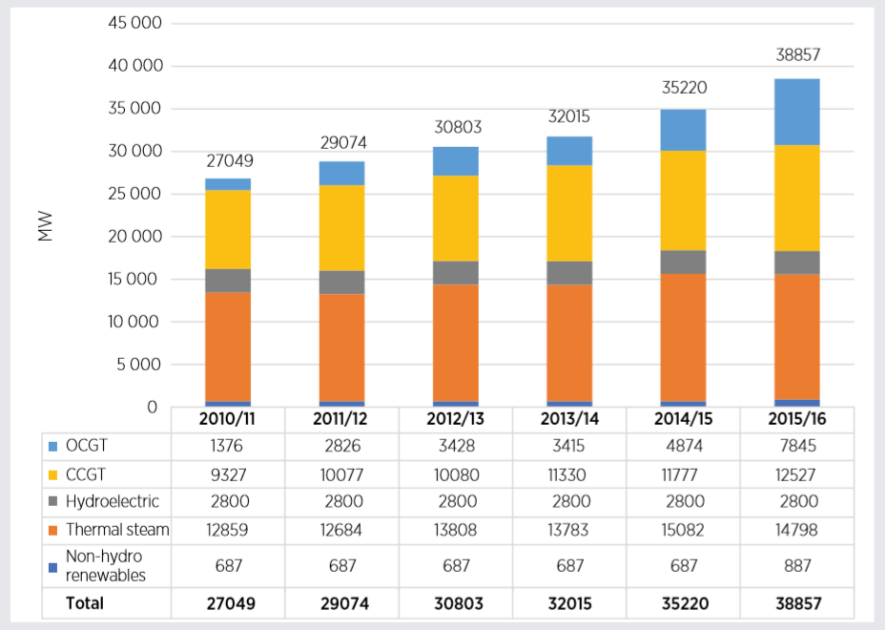

	2010/11	2011/12	2012/13	2013/14	2014/15	2015/16
OCGT	1376	2826	3428	3415	4874	7845
CCGT	9327	10077	10080	11330	11777	12527
Hydroelectric	2800	2800	2800	2800	2800	2800
Thermal steam	12859	12684	13808	13783	15082	14798
Non-hydro renewables	687	687	687	687	687	887
Total	**27049**	**29074**	**30803**	**32015**	**35220**	**38857**

Figure 4.1 – Installed capacity of power plants by plant type [8]

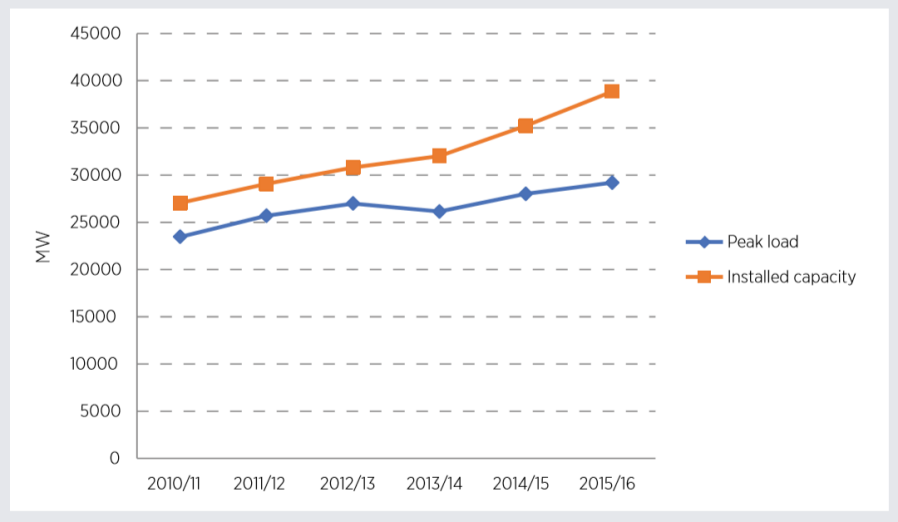

Figure 4.2 – Development of installed capacity and peak load [8]

Electricity is used by different end-users in the market. Out of the 156 300 GWh electricity consumption in 2015/16, they were split into residential (47%), industrial (25%) and commercial (12%), the remainder being used by industry, agriculture, public lighting and public utilities (4%) as shown in figure 4.3. [8]

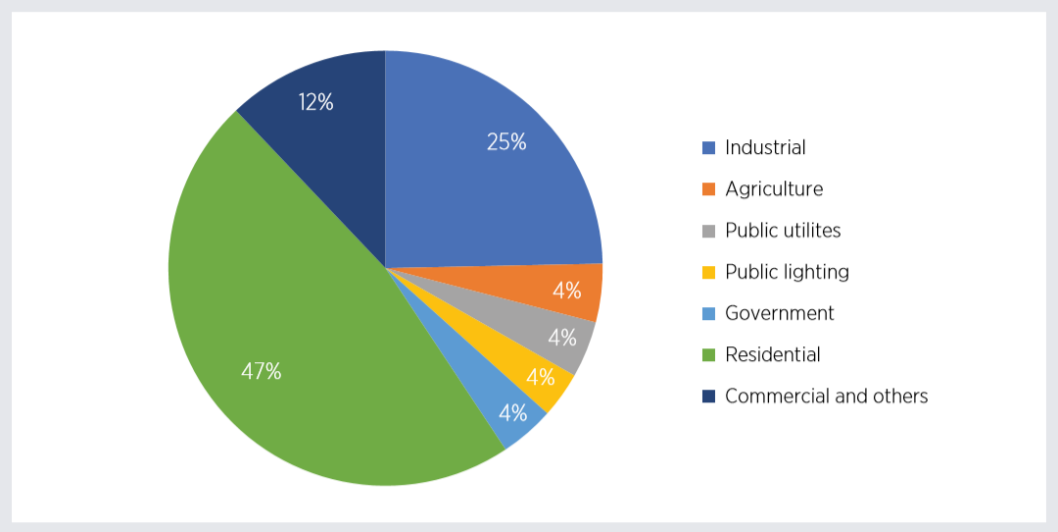

Figure 4.3 – Electricity consumption by sector [8]

Renewable energy development in Egypt is a major element in resolving the difficulties it faces in securing sufficient power generation due to uneven rates of gas output, and in resolving substantial rises in carbon dioxide (CO2) emissions.

4.1 Energy sources in Egypt

Endowments of fossil fuel energy supplies (including oil, natural gas, and small volumes of low-coal) are restricted in Egypt. At the end of 2014, overall proven oil reserves (crude oil and natural gas) were approximately 14.8 billion barrels (bbl) of oil equivalent, of which 3.4 billion bbl were in the form of crude oil and approximately 11.4 billion as natural gas (equivalent to 64 trillion cubic feet of natural gas)

Egypt enjoys an array of renewable energy options–solar, wind, biomass and hydro, despite the diminishing fossil fuel supplies. Average daily sunshine totals about 9 to 11 hours per day, with solar direct radiation intensity of about 2000 - 3200 (kWh/m²) per year which can be used for power production and thermal applications. Furthermore, Egypt is blessed with large wind energy, with average annual speeds exceeding 8–10 (m/s) along the Red Sea coast and 6–8 (m/s) along the coasts of the Southwest Nile and in the South of the Western Desert, which can be used for electricity production. More than 30 million tons of solid biomass wastes are also generated from both agriculture and municipal resources every year. Given an abundance of sustainable sources such as biomass, hydro, wind, and solar, the considerable capacity for harnessing electricity from such sources remains untapped. [8]

4.2 Renewable energy contribution to installed power capacity

The cumulative installed capacity of renewable energy sources is expected to reach 19.2 GW by 2021/22 and rise to 49.5 GW and 62.6 GW respectively in years 2029/30 and 2034/35. The table below demonstrates the growth of installed electric capacity for various renewable technologies between 2009 and 2035.

Table 4.1 - Installed electric capacity for various renewable technologies between 2009 and 2035. [8]

Type of power station	2009/10	2021/22	2029/30	2034/35
Hydro	2.8	2.8	2.9	2.9
Wind	0.5	13.3	20.6	20.6
Photovoltaics	0.0	3.0	22.9	31.75
Concentrated Solar Power	0.0	0.1	4.1	8.1
Total	**3.3 GW**	**19.2 GW**	**50.5 GW**	**62.6 GW**

4.3 Renewable energy potential and use

4.3.1 Hydroelectric energy

The largest hydro-resource in Egypt is the River Nile, with the maximum capacity in Aswan, where a total of 2 800 MW of power stations are situated, with corresponding annual electricity production of 13 545 GWh. In the 1960s and 1970s, hydroelectricity accounted for almost 50% of the total electricity produced by Egypt. Nonetheless, due to the rise in the proportion of thermal power plants, hydroelectricity accounted for just 7.2% of the overall electricity produced in 2015/16.

Hydropower is the most advanced clean energy technology in Egypt, with an average growth rate of 1.2% per year in electricity produced from hydropower projects between 2011/12 and 2015/16. The breakdown of hydroelectric stations by 2015 is depicted in table 4.2.

Table 4.2 - Breakdown of hydroelectric stations by 2015 [8]

Station	Capacity (MW)	Annual generated electricity (GWh)
High dam	2 100	9 484
Aswan 1	280	1 578
Aswan 2	270	1 523
Esna	86	507
Naga Hamady	64	453
Total	**2 800**	**13 545**

A further four hydroelectric plants with a capacity of 32 MW are being constructed at Assiut, Upper Egypt. Moreover, plans for the building of a 2 400 MW pumped storage hydroelectric power plant at Attaqa were launched in 2015, scheduled to be completed in 2022. The plant is expected to run at peak hours, based on water flowing from an upper reservoir to a lower one with a 28 meter height difference. The flow is reversed during the off-peak period, and the upper reservoir is typically refilled by using the turbines as pumps and the generators as motors. The electricity required for the motor generators to work is provided by the surplus power available during off-peak times.

4.3.2 Wind energy

The country is endowed with plentiful wind energy resources, especially in the Gulf of Suez region, according to Egypt's Wind Atlas (Wind Atlas for Egypt Measurement and Modelling 1991-2005). Because of its high steady wind speeds, which cross on average between 8 and 10 m/s at a height of 100 meters, this is one of the best places in the world for harnessing wind energy, along with the existence of large uninhabited desert areas.

In addition, promising new regions in the Beni Suef and Menya Governorates and El Kharga Oasis in the New Valley Governorate were discovered east and west of the Nile. They deliver wind speeds ranging from 5 to 8 m/s, and are ideal for wind power generation and other applications such as water pumping. Figure 4.4 introduces the latest wind atlas on IRENA's Global Atlas platform, posted in 2016.

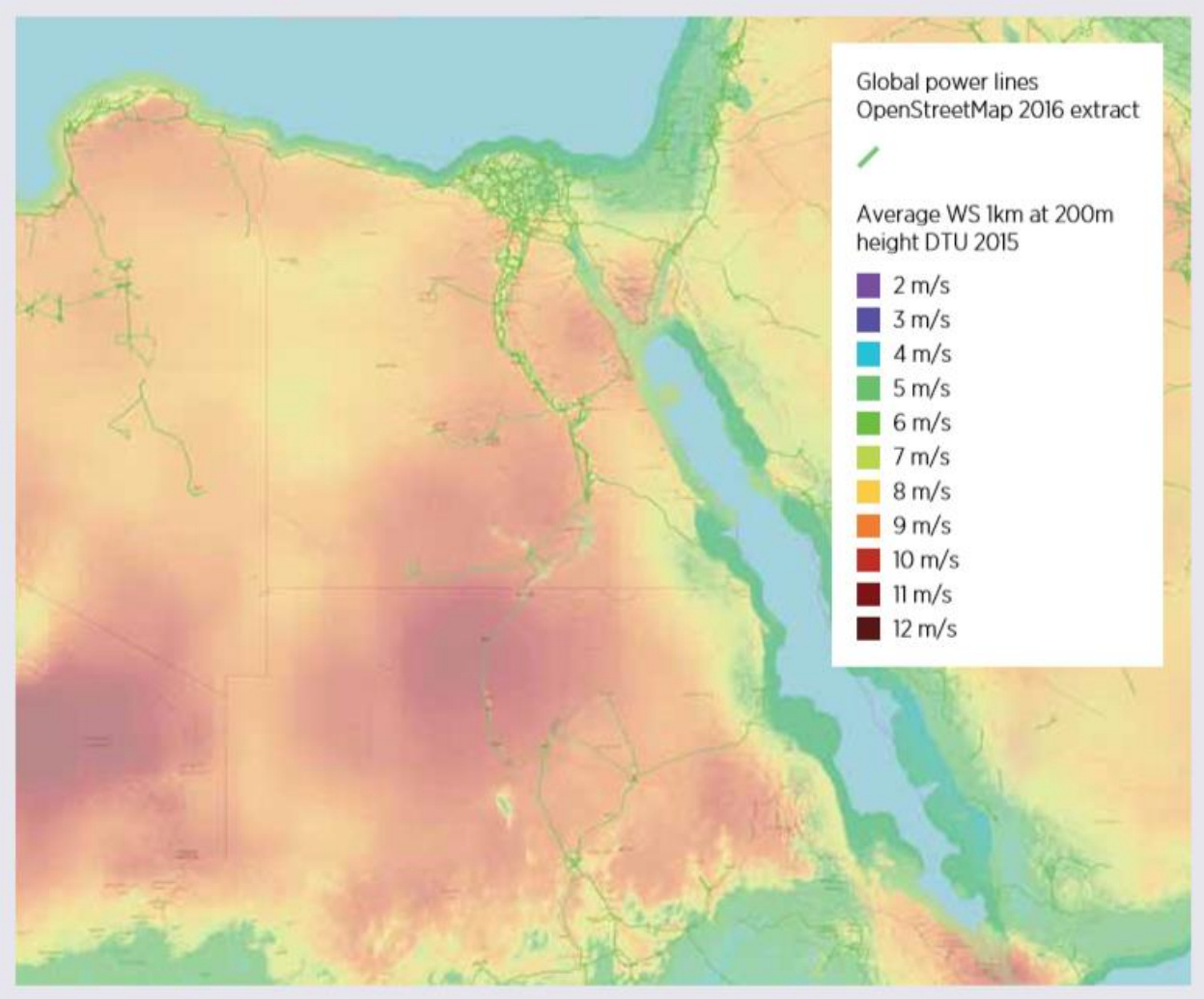

Figure 4.4 – Egypt's wind atlas [8]

In 1993, the first wind farm in Egypt was built in Hurghada, with 42 units with various technology and a total capacity of 5.2 MW. Since 2001, the NREA has built, in partnership with Germany, Spain, Japan and Denmark, a series of large-scale wind farms totalling 545 MW in 2010/11, increased to 750 MW in November 2015, under an engineering, procurement and construction (EPC) scheme in both Zaafarana (545 MW) and Gulf of El Zayt (200 MW).

This installed capacity corresponded to total windgenerated electricity ranging from 260 GWh in 2001/02 to 2 058 GWh in 2015/16. As a result of the use of wind energy for power generation, gross traditional fuel consumption rose from 58 Mtoe in 2001/02 to 432 Mtoe in 2015/16. Consequently, the CO2 emissions avoided in 2001/02 was measured at 143 000 tons and in 2015/16 at 1,131 million tons. Figure 4.5 outlines the evolution of wind-generated electricity in Egypt over the past few years.

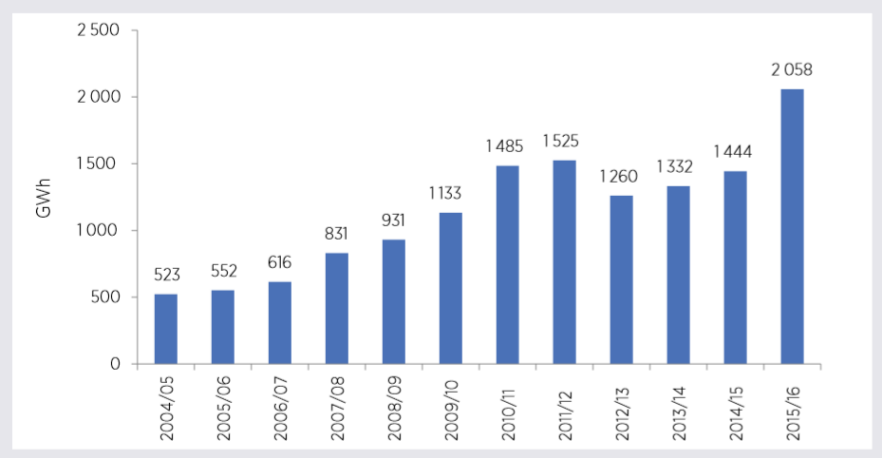

Figure 4.5 – Wind-generated electricity from 2004/05 to 2015/16 [8]

Four wind power plants are expected to be constructed and operating by 2023, with a combined installed capacity of 2 610 MW. Additionally, Siemens is developing 2 000 MW capacity of wind energy projects. Table 4.3 shows for more information on the proposed wind projects up to 2023.

Table 4.3 - Proposed wind projects up to 2023 in Egypt [8]

Project	Technology	Status	Size	Contract
Gulf of Suez	Wind	Under development	**250 MW**	NREA-KfW, EIB, AFD EPC scheme
Gulf of Suez	Wind	Under development	**250 MW**	GDF Suez, Toyota, Orascom BOO scheme
Gulf of Suez	Wind	Under development	**200 MW**	NREA-Masdar EPC scheme
Gulf of Suez	Wind	Under development	**200 MW**	AFD-KfW EPC scheme
Gulf of Suez	Wind	Under development	**2 000 MW**	Siemens EPC scheme
Gabal El Zayt	Wind	Under construction	**220 MW**	NREA-Japan-JICA EPC scheme
Gulf El Zayt	Wind	Under construction	**320 MW**	Italgen BOO scheme
Gabal El Zayt	Wind	Under construction	**120 MW**	Spain-NREA
West Nile-1	Wind	Under development	**250 MW**	BOO scheme
West Nile	Wind	Under development	**200 MW**	Japan EPC scheme
West Nile	Wind	Tender-bidding Phase	**600 MW**	NREA IPP scheme

4.3.3 Solar energy

Egypt has a favorable level of solar radiation. In 1991, the solar atlas for Egypt was released showing that the nation receives between 2 900 and 3 200 hours of sunlight yearly, with an annual direct normal intensity of 1 970-3 200 kWh/ m2 and a total intensity of radiation ranging from north to south of Egypt between 2 000 and 3 200 kWh/m2 per year as shown in figure 4.6. Globally, Egypt is one of the most desirable areas for the use of solar energy for both power production and thermal heating applications. [8]

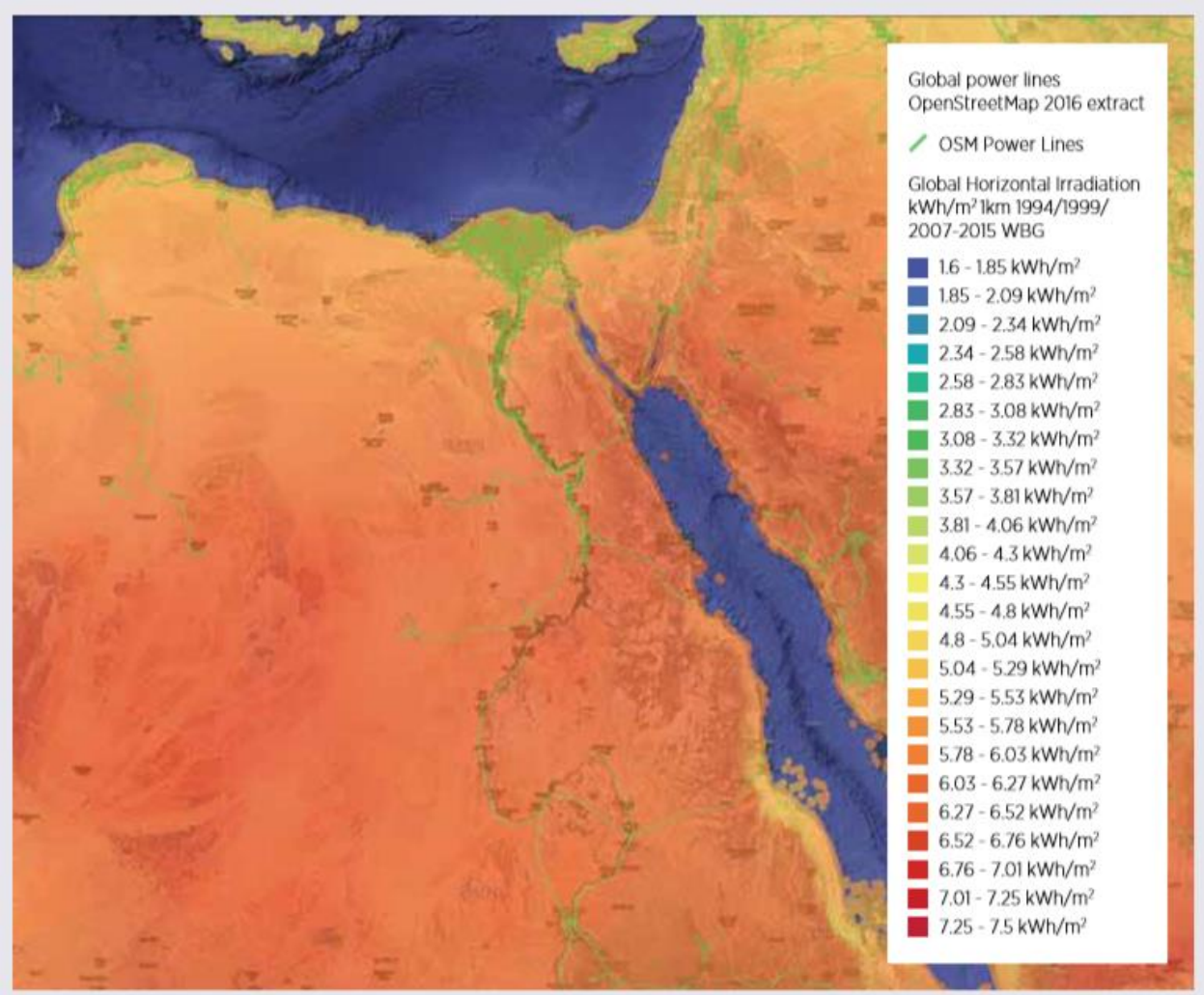

Figure 4.6 – Egypt's solar atlas [8]

Throughout 2013, the overall installed capacity of small-scale PV systems stood at 6 MW, and by the end of 2016 a combined 30 MW of off-grid power plants had been installed and operational. With the acceleration of Egypt's electricity scarcity in 2014, accompanied with the cost reduction of photovoltaic panels, many other Egyptian authorities have based their attention on implementing photovoltaic

applications, especially rooftop and street lighting systems. The following segment summarizes recent main accomplishments in that regard in Egypt.

4.3.4 Centralised grid-connected solar PV

The New and Renewable Energy Authority (NREA) has finalised feasibility studies for two large-scale PV plants with an installed capacity of 20 MW and 26 MW, respectively, to be constructed in Hurghada and Kom Ombo, and expected to be realised late in 2019. The former would be sponsored by JICA (Japan) and the latter by AFD (France). Each of them is projected to generate about 32 GWh and 42 GWh annually respectively, saving around 40 000 tons of combined CO2. Table 4.4 shows more information on proposed grid-connected projects.

Table 4.4 - Proposed grid-connected projects by 2015 in Egypt [8]

Project	**Type**	**Status**	**Size**	Contract
Kom Ombo	PV	Binding	200 MW	BOO scheme
West Nile	PV	Binding	600 MW	Sky Power and EETC BOO
West Nile	PV	Binding	200 MW	EETC BOO
West Nile	PV	Binding	600 MW	BOO scheme
FIT	PV	Operational	50 MW	EETC PPA
FIT	PV	Under development	1 415 MW	EETC PPA
Hurghada	PV	Tendering	20 MW	NREA-JICA EPC scheme
Zaafarana	PV	Under development	50 MW	NREA-JICA EPC scheme
Kom Ombo	PV	Under development	26 MW	NREA-JICA EPC scheme
Kom Ombo	PV	Under development	50 MW	NREA-JICA EPC scheme

4.3.5 Distributed solar PV

Development of distributed on-grid PV systems only started in mid-2014 with two government interventions on public buildings for rooftop PV systems, in which about 3 MW of PV systems were installed and connected to the distribution network.

In 2015/16 the NREA initiated multiple offgrid PV projects in collaboration with the United Arab Emirates for the electrification of remote villages with a total power of 32 MW, including 6,942 stand-alone systems totalling 2 MW; eight centralized systems totalling about 30 MW; plus street lighting systems and hybrid PV-diesel systems.

In addition to the cumulative 6 MW planned by 2013, many limited photovoltaic projects have been launched. So several programs in the works, distributed solar PV technologies are evolving fairly rapidly. With the elimination of power subsidies and growing tariffs, the business and exchange will combine small photovoltaic systems to meet the rising demand for energy and reduce their utility bills. [8]

4.3.6 Biomass

Egypt has substantial biomass wealth from agricultural waste, animal dung, and solid industrial waste. Agricultural waste amounts to approximately 35 million tons per year, 40 per cent of which is used for animal feeding, the remainder being used for energy purposes (equivalent to 5 Mtoe / year). Urban solid waste averages 0.5 kilograms per person per day, which in greater Cairo alone amounts to nearly 10 000 tons per day. In Egypt, various biomass technologies have been demonstrated, in particular for the development of animal waste biogas in rural areas, as well as for the processing and briquetting of agricultural waste. But these large resources have not yet been used for electricity production. [8]

5 Legislation and rules for connection of RES into the distribution grid [9]

Disturbances caused by local generation need to be reduced so that devices of other network users as well as DSO equipment would not be disturbed. Such impacts need to be analyzed based on methods for evaluating disturbances and acceptable limits.

Generation can be connected without need for disturbance evaluation provide that ration between network short circuit power (S_{kV}) and rated power of whole equipment (S_{rA}) is higher than 500.

If equipment is tested by recognized agency, connection assessment can utilize more favorable factor S_{kV}/S_{rG} (<500). Certification, test report, etc. regarding the expected disturbances need to be provided in case of wind generation.

Particular evaluation of connection of one or several generation at one point of connection need to be based on following limits:

A. Voltage change

- ΔU ≤ 3% Un (for joint point of connection in LV network);
- ΔU ≤ 2% Un (for joint point of connection in MV network and 110 kV)

B. Flicker

LONG-TERM FLICKER

For evaluation of one or several generation at point of connection, regarding the voltage variation causing the flicker, limit value needs to be at LV and MV joint point of connection

$$P_{lt} \leq 0.46$$

and for 110 kV joint point of connection

$$P_{lt} \leq 0.37$$

Long-term flicker (Plt) of single generation can be determined using the flicker factor c as:

$$P_{lt} = c \cdot \frac{S_{nE}}{S_{kV}}$$

where S_{nE} is rated power of equipment (S_{nG} for wind generation).

If the value calculated from the equation mentioned above is higher than 0.46, phase angles can be included and following equation can be used:

$$P_{lt} = c \cdot \frac{S_{nE}}{S_{kV}} |\cos(\psi_{kV} + \varphi_i)|$$

Note: If the test report of equipment contains the calculated flicker factor c for network impedance angle ψ thus only c_ψ is determined then this flicker value is used. Then it needs to be taken into account that cos part of equation is not in regarded in such case (or is equal to 1).

C. Harmonics currents

Harmonics are generated mostly by equipment that contains inverters or frequency converters. Harmonic currents emit by such equipment has to be specified by manufacturer in e.g. type test report.

Generation in MV network

Allowed overall harmonic currents for single MV point of connection can be calculated by multiplying referential currents ($i_{v\,pr}$), given in table 5.1, with short circuit power at joint point of connection.

$$I_{v\,pr} = i_{v\,pr} \cdot S_{kV}$$

In case of several equipment connected to the joint point of connection, acceptable each equipment harmonic currents are calculated by multiplying of overall harmonic currents with rate of apparent power of equipment (S_A) and overall connectable/planned power (S_{AV}) at joint point of connection

$$I_{v\,pr} = I_{v\,pr} \cdot \frac{S_A}{S_{AV}} = i_{v\,pr} \cdot S_{kV} \cdot \frac{S_A}{S_{AV}}$$

Substitution of ΣS_{nE} instead S_A can be used for equipment consisting of multiple modules of the same class. Such substitution works for wind generation as well. In case of equipment of various classes this is rough estimation though.

Table 5.1 provides overall acceptable harmonic currents that are related to short-circuit current and which are caused by equipment directly connected to the MV network.

In case of harmonic orders divisible by three, the closest order from Table 12 is valid unless the current zero sequence of generation is closing to the network.

Table 5.1 – Acceptable reference current of harmonic sources in MV network

Harmonic order (μ, ν)	**Acceptable reference current of harmonics $i_{\mu,\,\nu pr}$ [A/MVA]**		
	10 kV network	**22 kV network**	**35 kV network**
5	0.115	0.058	0.033
7	0.082	0.041	0.023
11	0.052	0.026	0.015
13	0.038	0.019	0.011
17	0.022	0.011	0.006
19	0.016	0.009	0.005
23	0.012	0.006	0.003
25	0.01	0.005	0.003
>25 or even	0.06/ ν	0.03/ ν	0.017/ ν
μ < 40	0.06/ μ	0.03/ μ	0.17/ μ
μ > 40	0.16/ μ	0.09/ μ	0.046/ μ

For sum of harmonic currents generated by both various consumers and generations applies following rules:

- Rectifiers governed by network (6 or 12 pulses)
  For harmonics that are abnormal for the rectifiers (v < 7) as well as for those that are normal for rectifiers (5^{th}, 7^{th}, 11^{th}, 13^{th} etc.), arithmetic sum can be used

$$I_\nu = \sum_{i=1}^{n} I_{\nu\, i}$$

  For abnormal higher order harmonics (v > 7), the overall harmonic current of given order is determined as root of sum of power of two of harmonic currents of given order.

$$I_\nu = \sqrt{\sum_{i=1}^{n} I_{\nu\,\mathrm{i}}^2}$$

- Pulse modulated inverters
  For μ order that is not integer on general but for values μ > 11 contains integer values as well, the overall current is equal to the root of sum of order of two for each equipment.

$$I_\mu = \sqrt{\sum_{i=1}^{n} I_{\mu\,\mathrm{i}}^2}$$

  If there are any abnormal harmonic currents of order μ < 11 then they are summed arithmetically.

More detailed evaluation is required if acceptable values of harmonic currents (or acceptable inter-harmonic currents) are violated. It must be taken into account that acceptable values of harmonic currents are chosen so they will be valid even for higher frequencies for inductive impedance of network i.e. for mostly overhead network. In networks with high penetration of cables, the network impedance is lower in many cases thus, higher harmonic currents can be acceptable. Presumption is the calculation and evaluation of harmonics voltage at joint point of connection while the real (frequency based) network impedance at given point is taken into account. Additionally to all given requirements, voltage shall not violate 0.2 % at frequency between 2 000 Hz and 9 000 Hz.

If there are multiple points of connection, the evaluation of one point of connection has to take into account all other point of connection. MV network state is considered to be acceptable provide that harmonic currents emitted into the network at each and every point of connection not violate following value:

$$I_{v\,V\,pr} = i_{v\,pr} \cdot S_{kV} \cdot \frac{S_{AV}}{S_s}$$

where:

***S_{AV}*:** the sum of injected apparent powers of all equipment at given joint point of connection

S_s: the overall power the network is designed for

If acceptable harmonic currents are violated based on this calculation, the connection is allowed only if more detailed calculation proofs that harmonics voltage levels in network are not violated.

For network voltages different from those provided by Table 5.1, reference harmonic currents can be calculated from values given in that table (inverse proportion).

More detailed harmonic calculates needs to be done if acceptable values of harmonic currents are violated.

6 Case Study: Is it possible to connect Wind Power plant Vestas V-90 2MV into the MV distribution network system in the point of common coupling (PCC)?

6.1 Description of a doubly-fed induction generator (DFIG) wind power plant

Among the different applied wind energy conversion systems (WECS) configurations, in this section we we will discuss a form where a variable speed turbine is connected through a gearbox to a wound rotor induction (WRIG). The rotor output is however fed to the grid through a partially rated frequency converter. This is also referred to as the doubly fed induction generator (DFIG). The DFIG's merits make it one of WECS' most commonly used generators. The DFIG WECS have been in use for many years now in wind power generation, and have a major share of the global market. In this case study we will be using the Vestas V-90 which is a DFIG power plant. [10]

The DFIG WECS is a mixture of aerodynamic, mechanical, electromagnetic, and electronic systems, and as such, the control of the various subsystems in both steady and transient states is quite complex, especially since the increase in wind power penetration has resulted in more stringent grid codes which specify that the WECS must remain connected to the system even when a fault occurs and, furthermore, must provide

reactive currents to support the grid voltages. This is made more difficult by the intermittent and uncertain nature of the prime mover, the wind.

6.1.1 Construction

The DFIG WECS consists of a wind turbine (WT) system connected to a DFIG through a gearbox for the purpose of collecting mechanical power from the air flows and transforming it into electrical power. The output of the wind turbine increases as the wind speed cube increases. Wind speed increases with increase in altitude. The generator, gearbox and related control devices are located in a nacelle on the top of the tower. The main components of the wind turbine are shown in figure 5.1. [10]

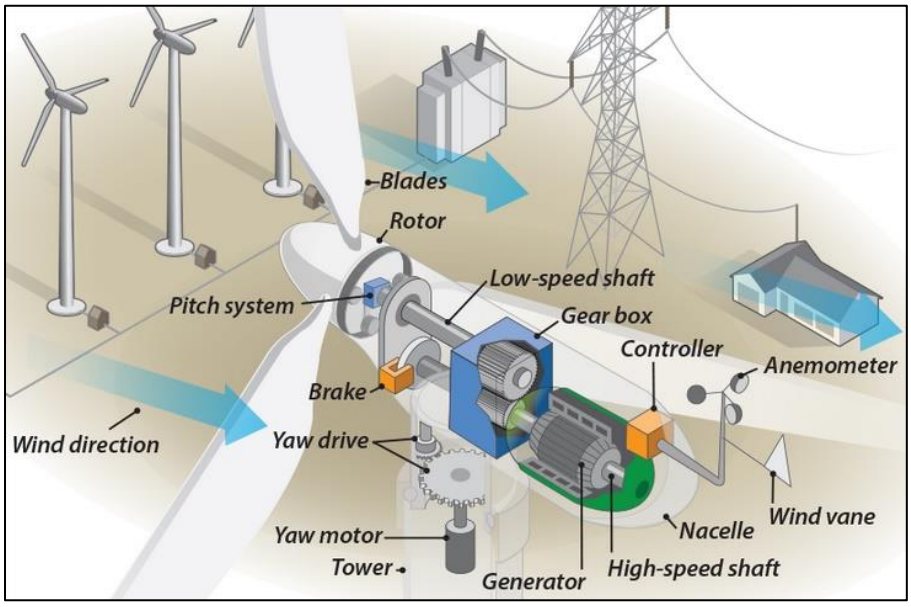

Figure 6.1 – Main components of a wind turbine [4]

The DFIG wind energy conversion systems (WECS) utilizes three bladed horizontal axis wind turbines with active blade pitch capability. The DFIG has a wound stator composed of three copper windings with a 120◦ spatial offset in two pole generators, while those with four poles have six offset windings at 60◦. The stator is connected to the grid bus, either directly or via a transformer, depending on the level of its output voltage in relation to the grid voltage. It also has a wound rotor which is brought out through slip rings and carbon brushes for connection to a power electronic converter (PEC) and then either directly or through a transformer, to the stator terminals.

The components in the rotor circuit include the following:

- ***dv/dt Filter***. It is a parallel resistance to an inductance linked between the rotor winding terminals and the rotor side converter (RSC) terminals to protect the rotor windings from adverse RSC

effects including bearing currents, capacitive leakage currents, and degradation of insulation due to the polarization effect by the resultant capacitive displacement current from sudden rise in voltage.

- ***Power Electronic Converter (PEC)***. It includes the following:
    - ***Rotor Side Converter (RSC)***. This is a voltage source converter (VSC) type, chosen over current source type because of its faster response to system changes and lower losses in the DC-link. It is composed of a rectifier bridge utilizing insulated gate bipolar transistors (IGBT) and diodes. It supplies magnetization current to the rotor. It also controls active and reactive generator power output by injecting currents of varying amplitude and frequency into the rotor windings. Slip power is also sent to the DC-link. The IGBTs switching is controlled by pulses generated by either sinusoidal pulse width modulation (SPWM) or space vector modulation (SVM) techniques.
    - ***Grid Side Converter (GSC).*** The GSC is a bidirectional rectifier bridge, using IGBTs as the switching tool, which is responsible for maintaining the DC bus voltage within certain limits by transmitting power, which is stored in the DC-link capacitor, from the rotor to the grid. It also exchanges reactive power with the grid either by receiving reactive power from the grid, or by exporting reactive power to the grid according to the set value. Its power factor is normally set to unity to minimize current flowing in it.
    - ***DC-Link***. It connects the RSC with the GSC as seen in figure 5.2. It consists of an energy storage capacitor or a mixture of multiple capacitors that aim to maintain constant voltage at their terminals. A VSC is characterized by a high value of capacitance in the DC-link.

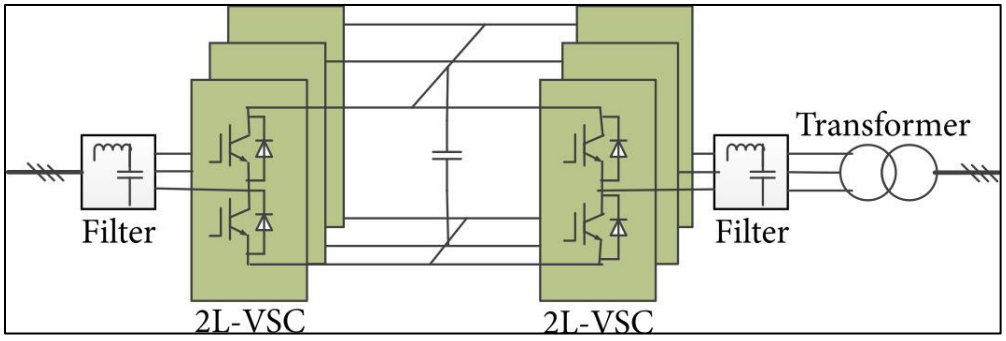

Figure 6.2 – Two-level back-to-back voltage source converter [10]

As the individual size of DFIG WECS increase, the high power ratings will result in different converter configurations to accommodate the high currents and voltages with existing semiconductor device ratings. In this paper, we will only be discussing one configuration: Two-Level Back-to-Back voltage soucre converters (VSC). It is the most established solution with a simple structure and few components. Bulky filters are required to limit the high dv/dt stresses on generator and transformer

due to the only two voltage levels and to reduce the total harmonic distortion (THD) of grid voltages and currents.

- ***Harmonic Filter***. The VSC produces harmonics, in multiples of the switching frequency, which cause the grid voltages and currents to be distorted. The harmonics can be minimized by using filters, either active, passive, or hybrid, and by control that utilizes RSC or GSC capacity.
- ***Electromagnetic Compatibility (EMC) Filter***. IGBTs switching on and off causes interference over a wide spectrum of signals. The interference signals can be transmitted or received by electrical connections through impedances between the emitting source and the susceptible equipment, through magnetic and electric fields causing capacitive and inductive connections, and by radiation. The EMC filter decreases such emissions to a level where it is possible to operate other electrical devices in the vicinity without problems. The PEC itself must also not be affected by low levels of external interference to avoid giving rise to cases of dangerous operating states.
- ***Converter Control Unit (CCU).*** It executes control of the different rotor circuit elements for synchronized, reliable , and accurate operation. The CCU is a programmable electronic device, with various inputs from its own measurements and the WECS controller, and it sends output signals to the controlled elements. It also has communication channels for remote sensing and control. Controls for the RSC and GSC under both normal conditions and grid disturbance conditions must ensure that predetermined setpoints are met.

6.1.2 Operation

The DFIG WECS is a variable speed wind turbine (VSWT) which operates at varying speeds corresponding to the varying wind speeds from the cut-in speed (Point A) to the rated wind speed (Point C) to the cut-out speed (Point E), as shown in the turbine torque characteristic curves figure 5.3. [10]

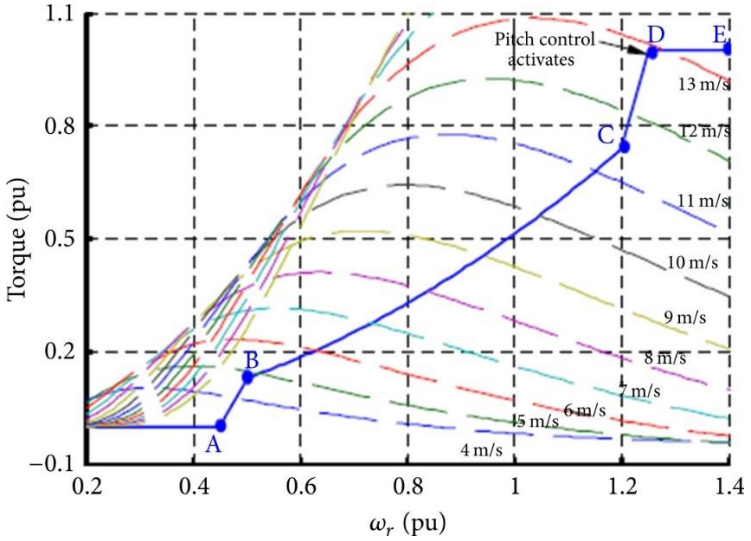

Figure 6.3 – Turbine torque characteristics [10]

The machine is at a standstill when below cut-in speed (point A), since the wind speed is too weak for effective and economical operation. When there is enough wind, the rotor begins to rotate, and the machine begins to generate power. The power coefficient is maintained constant at its maximum between points B and C to maximize power output as the wind speed increases. This is done by applying a maximum power point tracking (MPPT) strategy which adjusts the turbine rotor speed in realtion to the prevailing wind speed. The blade pitch angle is set at 0◦ during this period. Beyond point D, power regulation is introduced to ensure output power does not surpass rated power as wind speed continues to increase. The power coefficient is lowered by pitching the rotor blades, hence reducing the turbine rotating speed. At the cut-out speed, point E, the machine is stopped by pitching the turbine blades out of the wind and deploying the emergency brake to avoid structural damage due to high wind speeds. Running at high speeds can also result in high noise emission. [11]

Although DFIG WECS has been used in stand-alone applications, supplying power to the grid is the most popular use. The DFIG stator draws a reactive magnetizing current that is either provided by the grid or the GSC. Since the DFIG is an asynchronous generator, its electromagnetic torque is developed when currents induced in the rotor windings set up a magnetic field which interacts with the stator field. Both the voltage induced by the rotating stator field and the voltage supplied by the RSC induce these currents in the rotor. The stator field is of constant frequency set by the grid frequency. On the other hand, the rotor field is of variable frequency that relies on the slip. The bidirectional power transfer in the PEC enables two modes of operation:

(i) Subsynchronous mode or partial load mode at below rated speeds: the stator of the DFIG supplies power to the grid and slip power to the rotor via the converters and slip rings.
(ii) Supersynchronous mode or nominal load range at above rated speed: both the stator output power and the rotor slip power are fed to the grid.

6.1.3 Advantages and Disadvantages

The DFIG WECS has the following advantages:

(i) Higher efficiency even at low wind speeds
(ii) Decoupled control of active (P) and reactive (Q) powers, hence being more responsive to system needs
(iii) Reduced acoustic noise making the system more environmentally acceptable
(iv) Reduced mechanical stresses which reduces maintenance costs and prolongs system lifetime
(v) Contributing to system power quality improvement without using external reactive compensation devices
(vi) Less cost as PEC is rated for lower power levels, usually 30%

And it has the following disadvantages:

(i) The direct connection of the stator to the grid leaves the machine more vulnerable to system disturbances such as voltage dips and swells as the partially rated VSC is limited in its ability to withstand over currents and over voltages induced in it by stator fault currents due to the magnetic coupling between the stator and the rotor.

(ii) The VSC is a source of harmonics due to switching actions.

(iii) Use of PEC, gearbox, and slip rings introduces increased costs and maintenance needs, increased losses, and decreased reliability as they increase the number of components that can fail.

6.1.4 Modelling

The DFIG WECS has two main subsystems. The first manages harnessing of energy in the airflows and the subsequent conversion into rotational mechanical power. This subsystem contains the turbine rotors, hub, low speed shaft, gearbox, and high speed shaft which is attached to the rotor generator. The second subsystem handles the conversion of the mechanical power into electrical power. This is handled by the generator and the PEC. [10]

I. Subsystem One: The Wind Turbine Model.

The mechanical power extracted from the wind is given by

$$\boldsymbol{P_m = \frac{1}{2}\, A\rho V^3 C_p\,(\lambda, \beta)} \quad [\boldsymbol{W}]$$

And the mechanical torque developed by the wind turbine shaft is given as

$$\boldsymbol{T_m = \frac{P_m}{\omega_m} = \frac{1}{2}\, A\rho V^2 C_p(\lambda, \beta)\frac{R}{\lambda}} \quad [\boldsymbol{N * m}]$$

Where the power coefficient is given by

$$\boldsymbol{C_p(\lambda, \beta) = 0.5(\Gamma - 0.02\beta^2 - 5.6)e^{-0.17\Gamma}}$$

Where Γ is equal to

$$\boldsymbol{\Gamma = \frac{R(3600)}{\lambda(1609)}}$$

Where,

$\boldsymbol{P_m}$	Mechanical power [W]
$\boldsymbol{T_m}$	Mechanical torque [N*m]
$\boldsymbol{A}$	Area swept by turbine rotor [m2]
$\boldsymbol{V}$	Wind speed [m/s]
$\boldsymbol{C_p}$	Power coefficient
$\boldsymbol{\rho}$	Air density [kg/m3]
$\boldsymbol{\lambda}$	Tip speed ratio (TSR), given as $(\omega_{\mathrm{m}} * R/V)$
$\boldsymbol{\beta}$	Blade pitch angle (degrees)
$\boldsymbol{\omega_m}$	Angular speed of wind turbine [rad/s], given as $(p\Omega_{\mathrm{m}}/2)$
$\boldsymbol{p}$	Number of poles
$\boldsymbol{\Omega_m}$	Rotor mechanical rotational speed [rad/s]
$\boldsymbol{R}$	Radius of turbine rotor [m]

II. Subsystem Two: The DFIG Model.

The DFIG park model in the d-q reference frame, assuming sinusoidal flux, constant winding resistance, and neglecting magnetic saturation, is given in figure 5.4.

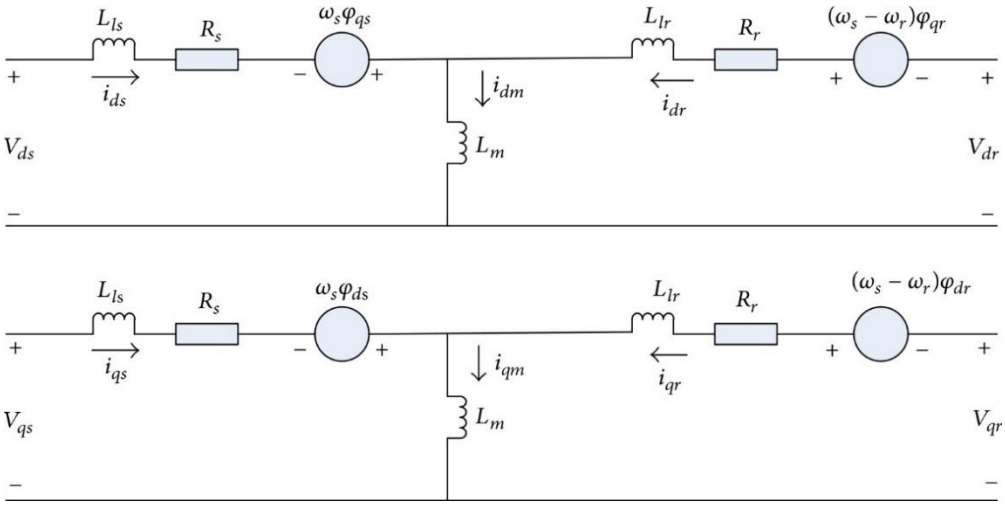

Figure 6.4 – DFIG equivalent circuit in d-q reference frame [10]

The equations relating the DFIG park model stator and rotor voltages and fluxes are

$$\boldsymbol{v_{ds} = R_s i_{ds} - \omega_s \varphi_{qs} + \frac{d\varphi_{ds}}{dt}}$$

$$\boldsymbol{v_{qs} = R_s i_{qs} + \omega_s \varphi_{ds} + \frac{d\varphi_{qs}}{dt}}$$

$$\boldsymbol{v_{dr} = R_r i_{dr} - \omega \varphi_{qr} + \frac{d\varphi_{dr}}{dt}}$$

$$\boldsymbol{v_{qr} = R_r i_{qr} + \omega \varphi_{dr} + \frac{d\varphi_{qr}}{dt}}$$

where v are voltages (V), i are currents (A), R are resistances (Ω), and φ are flux linkages (V·s). Indices d and q indicate direct and quadrature axis components, respectively, while s and r indicate stator and rotor quantities, respectively, and ω_s is grid electrical angular speed, ω_r is rotor electrical angular speed and slip speed, and ω is given by $\omega_s - \omega_r$.

The direct and quadrature stator and rotor flux components are decoupled magnetically and are given by

$$\boldsymbol{\varphi_{ds} = L_s i_{ds} + L_m i_{dr}}$$

$$\boldsymbol{\varphi_{qs} = L_s i_{qs} + L_m i_{qr}}$$

$$\boldsymbol{\varphi_{dr} = L_r i_{dr} + L_m i_{ds}}$$

$$\boldsymbol{\varphi_{qr} = L_r i_{qr} + L_m i_{qs}}$$

where $L_s = L_{ls} + L_m$ and $L_r = L_{lr} + L_m$, L_{ls} and L_{lr} are stator leakage and rotor self-inductances, and L_m is mutual inductance (H).

The equivalent circuit for the grid side converter connection to the grid is given in figure 5.5. The voltage across the inductor is given, in the d-q reference frame, by

$$\boldsymbol{v_{gd} = R_g i_{gd} + L_g \frac{di_{gd}}{dt} - \omega_s L_g i_{gd} + v_{gcd}}$$

$$\boldsymbol{v_{gq} = R_g i_{gq} + L_g \frac{di_{gq}}{dt} - \omega_s L_g i_{gq} + v_{gcq}}$$

Where V_{gcd} and V_{gcq} are voltages at GSC output terminals while V_{gd} and V_{gq} are voltages at the grid.

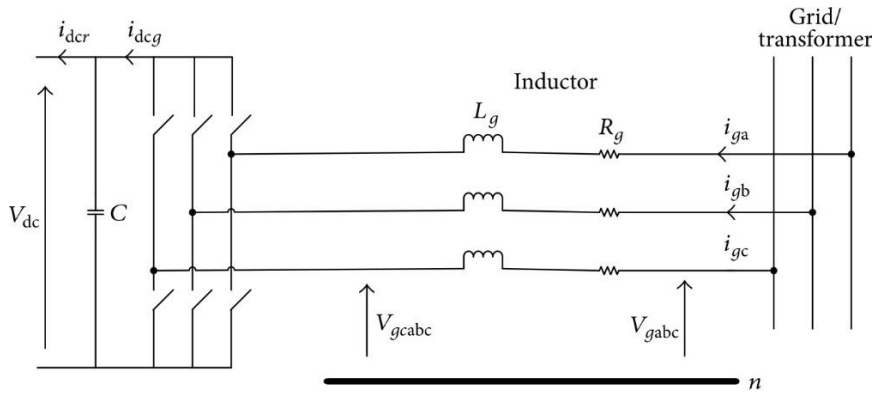

Figure 6.5 – Schematic of GSC connection to grid [10]

6.1.5 Faults

The main challenge in operation of the DFIG WECS is continued operation under fault conditions. Faults may originate from the machine internally, or from the grid externally. Table 6.1 gives a summary of the internal faults, their effects, and solutions proposed. More than 50 percent of internal faults are attributed to the PEC with 30 percent arising from the DC-link capacitor. More than 50 percent of internal faults are attributed to the PEC with 30 percent originating from the DC-link capacitor. While the gearbox accounts for just 5 percent of failures, it is generally more expensive, often requiring complete replacement of the gearbox, leading in more downtime.

Table 6.1 - Internal faults, their effects, and proposed solutions [10]

Component affected	Effect	Causes	Risk	Solutions
Turbine	Balde fracture	Excessive loading from wind gusts or icing	Blade pieces and dislodged ice flying off risking damage to other turbines and personnel	Emergency shutdown in high gust or ice situations Deicing systems incorporated in rotor blades
	Lighting strike	Strikes by lightning	Fire	Lightning earthing system incorporated in rotor blade
	Hydraulic failure	Control system malfunction, environmental degradation	Loss of timely control Fire from leaking oil	Timely preventive maintenance

Gearbox	Gearbox failure	Insufficient lubrication	Worn or fractured gears, fire	Use of sufficient and correct high quality lubricants Sufficient lubricant cooling system
Generator	Windings open circuit, winding insulation failure	High operating temperatures, transient voltages and currents	Reduced or stoppage of power production	Regulation of voltages and currents to ensure stable operating temperatures
PEC	Semiconductor device failure Failure of bond wire connection	Thermal cycling	Output power fluctuations	Control that reduces thermal variations
	DC-link capacitor failures	Voltage fluctuations, harmonic currents	Reduced output power, increased fluctuations in output currents	Control that reduces voltage variations across the capacitor

6.2 DNCalc Application [14]

DNCalc application is used for modeling and complex analysis of large, meshed and parallel operated networks (LV, MV and HV). Key features are as follows:

- Analysis are based on D-A-CH-CZ, EN 50160, EN 60909-0, EN 60909-1, EN 60909-3, IEC 1000-2-2, EN 61000-3-2, EN 61000-3-3, 61000-3-4, EN 61000-4-30, PNE 33 3430 standards and others [15] [16] [17]
- Tools for evaluation of load and generation connectivity from DS point of view;
- Tools for power quality analyzation;
- Three-phase or four-lines models allow evaluation of each phase;
- Analysis of power networks over map background; open platform for information import from GIS for creating and updating of modeled distribution networks;
- Supports online calculations and transferring results to other DSO's systems and applications if they are interconnected;
- Smart Grid analysis;
- Power supply reliability – it is supported by TA CR – switching elements, reconstructions, cable systems, DS status improvements, forest paths, maintenance coordination, SAIDY, SAIFI (MAIFI) reliability indicators, rate of investment return, etc.;
- The area of dynamics – static and dynamic steadiness (under development)

6.3 Study of connectivity

In this case study, our main goal is to evaluate connectivity of a wind power plant **(Wind Vestas V90)** with installed capacity 2MW to distribution network 22kV from the perspective of voltage change and flicker effect. Figure 5.6 illustrates the network scheme. All of the analysis and calcutation has been done using DNCalc software. [12]

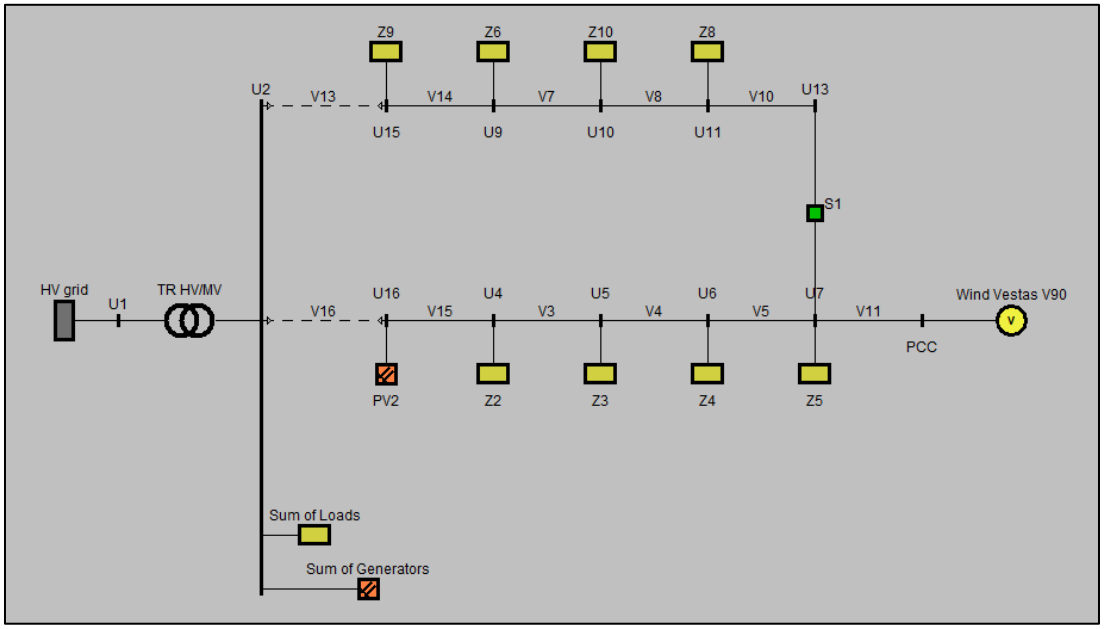

Figure 6.6 – Network scheme

The HV network is represented by Power supply node (HV grid) with short circuit power ratio and R/X ratio, nominal voltage is 110 kV, operated voltage is 115 kV. Power grid is assumed as symmetrical (voltages at each phase are the same, load and generation is symmetrical).

Supply node	Un [kV]	Uop [kV]	Isc [kA]	Ssc [MVA]	R/X	R0/R1	X0/X1
HV grid	110	115, 115, 115	4.19891	800	0.15	1	1

The MV distribution network is supplied by HV/MV transformer with tap changer. Transformer model is based on ČSN 60909-0, PI model with internal T-section is used [13]

	Un1 [kV]	Un2 [kV]	St [MVA]	Pk [kW]	uk [%]	I0 [%]	P0 [kW]
Transformer (TR HV/MV)	110	23	25	140	11	0.34	27
	Primary	**Secondary**	**Tap changing**	**Number of taps**	**Step [%]**	**In1 [A]**	**In2 [A]**
	YN	YN	●	8	2	131	628

The network contains two feeders and the rest of feeders can be assumed as “Sum of Loads” and “Sum of generation” and can be connected to the MV busbar (power lines can be neglected).

Several HV/MV distribution transformer stations (DTS) are added to the scheme. They are modelled as loads connected directly into the nodes along the power lines. Models of MV/LV transformers are neglected. Specific load profile of each load is described in the table below.

Load	Un [kV]	I [A]	cos ϕ	P [kW]	Q [kVAr]	S [kVA]
Sum of Loads	22	183.702	0.97	6790	1701.73	7000
Z10	22	1.78858	0.968392	66	17	68.1542
Z2	22	8.08444	0.973841	300	70	308.058
Z3	22	3.37355	0.972387	125	30	128.55
Z4	22	3.37355	0.972387	125	30	128.55
Z5	22	18.4563	0.867367	610	350	703.278
Z6	22	1.78858	0.968392	66	17	68.1542
Z8	22	1.78858	0.968392	66	17	68.1542
Z9	22	8.08444	0.973841	300	70	308.058

Input parameters and types of overhead power lines are displayed in the following table. Overhead power lines and cables are modelled by PI section model.

Line	Type	Cross-section [mm²]	Un [kV]	R [Ω/km]	X [Ω/km]	B [µS/km]	Length [km]	Imax [A]
V10	35AlFe6	35	22	0.778	0.389	1.339	5	150
V11	35AlFe6	35	22	0.778	0.389	1.339	0.5	150
V13	120AXEKCY	120	22	0.253	0.219	75	1	307
V14	110/22AlFe6	110	22	0.259	0.368	1.46	5	318
V15	70/11-1AlFe6	70	22	0.431	0.383	1.431	5	225
V16	120AXEKCY	120	22	0.253	0.219	75	0.5	307
V3	70/11-1AlFe6	70	22	0.431	0.383	1.431	5	225
V4	70/11-1AlFe6	70	22	0.431	0.383	1.431	2	225
V5	50AlFe6	50	22	0.615	0.396	1.407	1	177
V7	50AlFe6	50	22	0.615	0.396	1.407	10	177
V8	50AlFe6	50	22	0.615	0.396	1.407	5	177

Input parameters of photovoltaic power plants are displayed in the following table.

Photovoltaic plant	Un [kV]	Sn [kVA]	Pn [kW]	cos ϕn	Poper [kW]	Qoper [kVAr]	cos ϕ oper
PV2	22	500	500	1	500	0	1
Sum of Generators	22	3000	3000	1	3000	0	1

The power source, 2MW wind power plant with power factor equal to 1, is connected into the point of common coupling (PCC) node. The table below shows the input nominal and operational parameters.

Asynchronous Machine	Un [kV]	Sn [kVA]	cos ϕn	R/X	Poper [kW]	cos ϕoper	k	cos ϕk
Wind Vestas V90	22	2000	1	1	2000	1	1.2	1

6.3.1 Calculation results

We will be testing the possibility of connection of the wind power plant (WPP) by finding results for the following calculations.

- Load-flow calculations
- Voltage change when the WPP is connected
- Short-term flicker (Pst parameter) for the best possible connection of the WPP to the grid.

First, we will have the following case to use as a reference:

- Case 1: Steady state (Wind power plant is disconnected)

Then, there will be two cases:

- Case 2: WPP is connected, Switch S1 is open
- Case 3: WPP is connected, Switch S1 is closed

1) STEADY STATE (Wind power plant is disconnected)

In this case, we will find Load-flow calculation in case of steady state of the WPP. The following tables will illustrate the voltage levels at each node and current distribution in branches (Overhead power lines and cables).

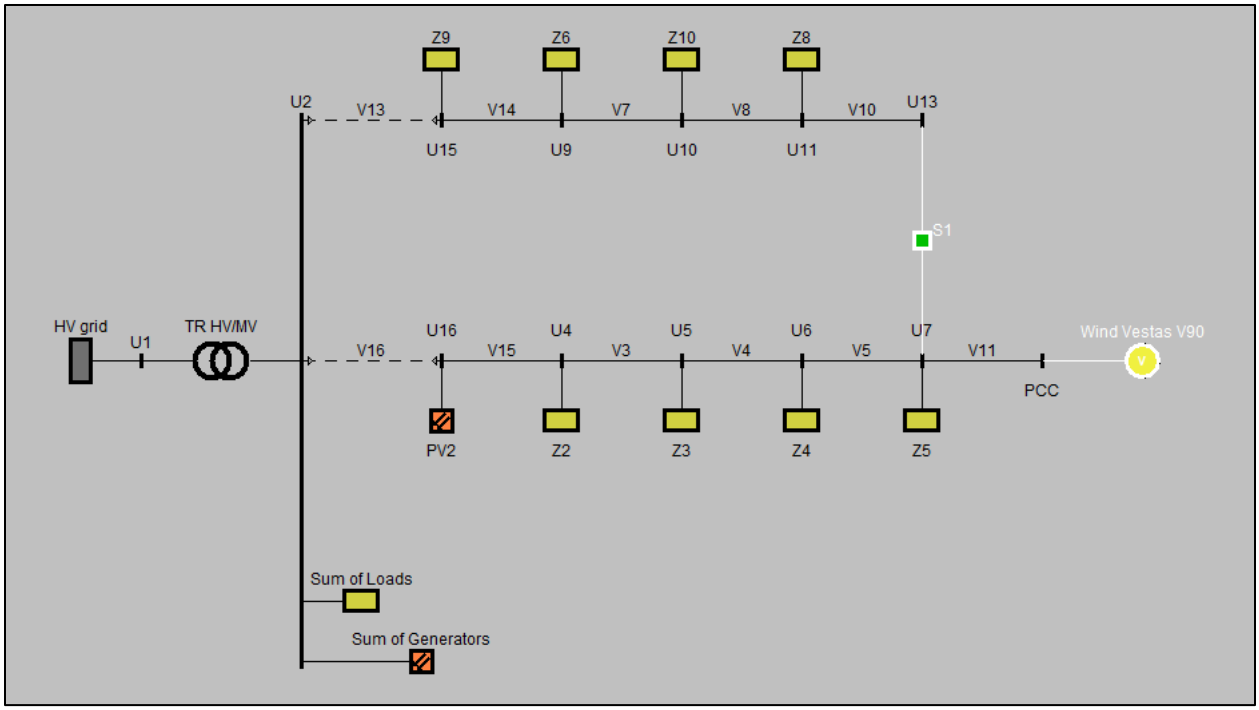

Figure 6.7 – Network scheme in case of the disconnection of the wind power plant

- **Conditions at nodes**

	Ua [kV]	αa [deg]	Ub [kV]	αb [deg]	Uc [kV]	αc [deg]	dUna [%]	dUnb [%]	dUnc [%]	Zk [Ω]	α [deg]	Sk [MVA]
U2	22,774	28,465	22,774	-91,535	22,774	148,465	-3,518	-3,518	-3,518	2,938	85,913	164,738
U1	114,582	29,699	114,582	-90,301	114,582	149,699	-4,165	-4,165	-4,165	15,125	81,467	799,997
U15	22,768	28,455	22,768	-91,545	22,768	148,455	-3,489	-3,489	-3,489	3,466	78,652	139,656
U9	22,753	28,42	22,753	-91,58	22,753	148,42	-3,425	-3,425	-3,425	7,062	66,275	68,534
U10	22,714	28,378	22,714	-91,622	22,714	148,378	-3,244	-3,244	-3,244	18,5	44,923	26,161
U11	22,704	28,367	22,704	-91,633	22,704	148,367	-3,198	-3,198	-3,198	24,495	41,915	19,759
U13	22,704	28,367	22,704	-91,633	22,704	148,367	-3,199	-3,199	-3,199	31,544	38,424	15,343
U16	22,768	28,463	22,768	-91,537	22,768	148,463	-3,49	-3,49	-3,49	3,195	81,985	151,468
U4	22,616	28,329	22,616	-91,671	22,616	148,329	-2,802	-2,802	-2,802	7,53	57,571	64,273
U5	22,499	28,242	22,499	-91,758	22,499	148,242	-2,269	-2,269	-2,269	12,222	51,367	39,599
U6	22,458	28,216	22,458	-91,784	22,458	148,216	-2,082	-2,082	-2,082	14,121	50,047	34,276
U7	22,435	28,213	22,435	-91,787	22,435	148,213	-1,978	-1,978	-1,978	15,289	48,69	31,657
PCC	22,435	28,213	22,435	-91,787	22,435	148,213	-1,978	-1,978	-1,978	15,963	47,71	30,32

- **Conditions at branches**

	Node	Ia [A]	αa [deg]	Ib [A]	αb [deg]	Ic [A]	αc [deg]	P [kW]	Q [kVAr]	S [kVA]
Sum of Loads	U2	177,46	-15,605	177,46	-135,605	177,46	104,395	6790	1701,73	6999,999
HV grid	U1	28,013	153,646	28,013	33,646	28,013	-86,354	-4994,55	-2441,7	5559,445
TR HV/MV	U1	28,013	-26,354	28,013	-146,354	28,013	93,646	4994,548	2441,702	5559,445
	U2	137,866	154,282	137,866	34,282	137,866	-85,718	-4960,96	-2227,8	5438,213
V13	U2	12,742	-8,895	12,742	-128,895	12,742	111,105	498,467	64,39	502,609
	U15	12,905	166,759	12,905	46,759	12,905	-73,241	-498,342	-103,17	508,91
V14	U15	5,1	-11,038	5,1	-131,038	5,1	108,962	198,342	33,169	201,097
	U9	5,116	167,902	5,116	47,902	5,116	-72,098	-198,241	-36,806	201,629
V7	U9	3,393	-10,098	3,393	-130,098	3,393	109,902	132,241	19,806	133,716
	U10	3,425	166,845	3,425	46,845	3,425	-73,155	-132,027	-26,939	134,747
V8	U10	1,697	-10,182	1,697	-130,182	1,697	109,818	66,027	9,939	66,771
	U11	1,713	166,766	1,713	46,766	1,713	-73,234	-66	-13,55	67,376
V10	U11	0,088	88,367	0,088	-31,633	0,088	-151,633	0	-3,451	3,451
	U13	0	0	0	180	0	0	0	0	0
V16	U2	20,679	-36,005	20,679	-156,005	20,679	83,995	672,488	461,678	815,712
	U16	20,962	142,884	20,962	22,884	20,962	-97,116	-672,323	-480,98	826,656
V15	U16	32,133	-23,844	32,133	-143,844	32,133	96,156	1172,323	480,98	1267,156
	U4	32,168	156,002	32,168	36,002	32,168	-83,998	-1165,64	-478,726	1260,118
V3	U4	24,437	-26,945	24,437	-146,945	24,437	93,055	865,641	408,724	957,282
	U5	24,477	152,857	24,477	32,857	24,477	-87,143	-861,774	-408,928	953,874
V4	U5	21,26	-28,975	21,26	-148,975	21,26	91,025	736,774	378,93	828,506
	U6	21,277	150,936	21,277	30,936	21,277	-89,064	-735,604	-379,336	827,653
V5	U6	18,085	-31,559	18,085	-151,559	18,085	88,441	610,604	349,338	703,473
	U7	18,094	148,391	18,094	28,391	18,094	-91,609	-610	-349,658	703,108
V11	U7	0,009	88,213	0,009	-31,787	0,009	-151,787	0	-0,337	0,337
	PCC	0	153,435	0	-90	0	180	0	0	0
Z9	U15	7,812	-14,679	7,812	-134,679	7,812	105,321	300	70,002	308,059
PV2	U16	12,679	178,463	12,679	58,463	12,679	-61,537	-500	0	500
S1	U13	0	0	0	0	0	0	0	0	0
	U7	0	0	0	0	0	0	0	0	0
Sum of Generators	U2	76,054	178,465	76,054	58,465	76,054	-61,535	-3000	0	3000
Z6	U9	1,729	-16,024	1,729	-136,024	1,729	103,976	66	17	68,154
Z10	U10	1,732	-16,067	1,732	-136,067	1,732	103,933	66	17	68,154
Z8	U11	1,733	-16,077	1,733	-136,077	1,733	103,923	66	17	68,154
Z2	U4	7,864	-14,805	7,864	-134,805	7,864	105,195	300	70,002	308,059
Z3	U5	3,299	-15,253	3,299	-135,253	3,299	104,747	125	29,999	128,549
Z4	U6	3,305	-15,28	3,305	-135,28	3,305	104,72	125	29,999	128,549
Z5	U7	18,098	-31,633	18,098	-151,633	18,098	88,367	610	349,995	703,276

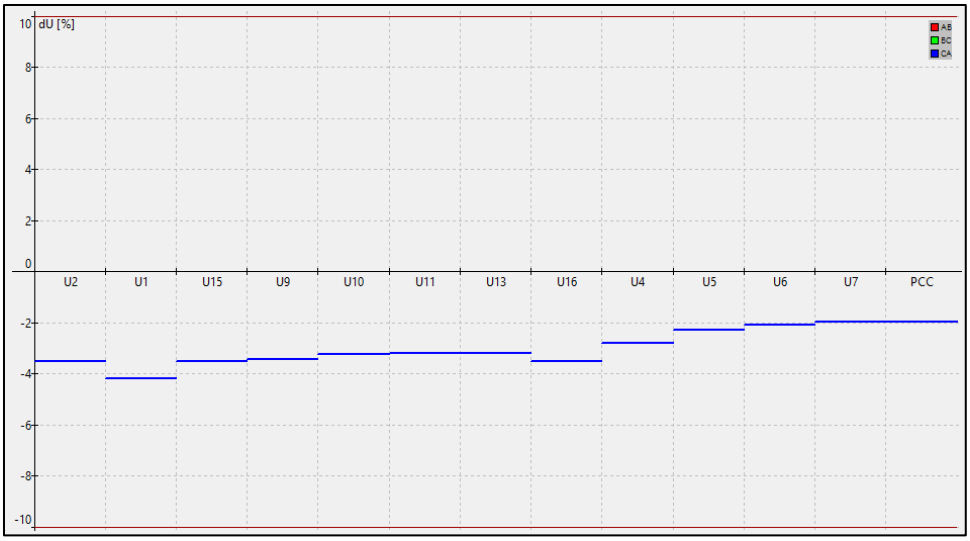

Figure 6.8 – Difference of voltage level (dU) from nominal voltage at each node

For the best results in voltage difference from the nominal voltage, TAP has been set as 2 (from an interval -8 to +8) at the transformer. From our tables and graphs, we can observe the voltage difference at each node from the nominal voltage. The highest difference is at node U1 **(4,165%)**, while the lowset difference is at nodes PCC and U7 **(1,978%)**.

2) 2MW WIND POWER IS CONNECTED, SWITCH S1 IS OPENED

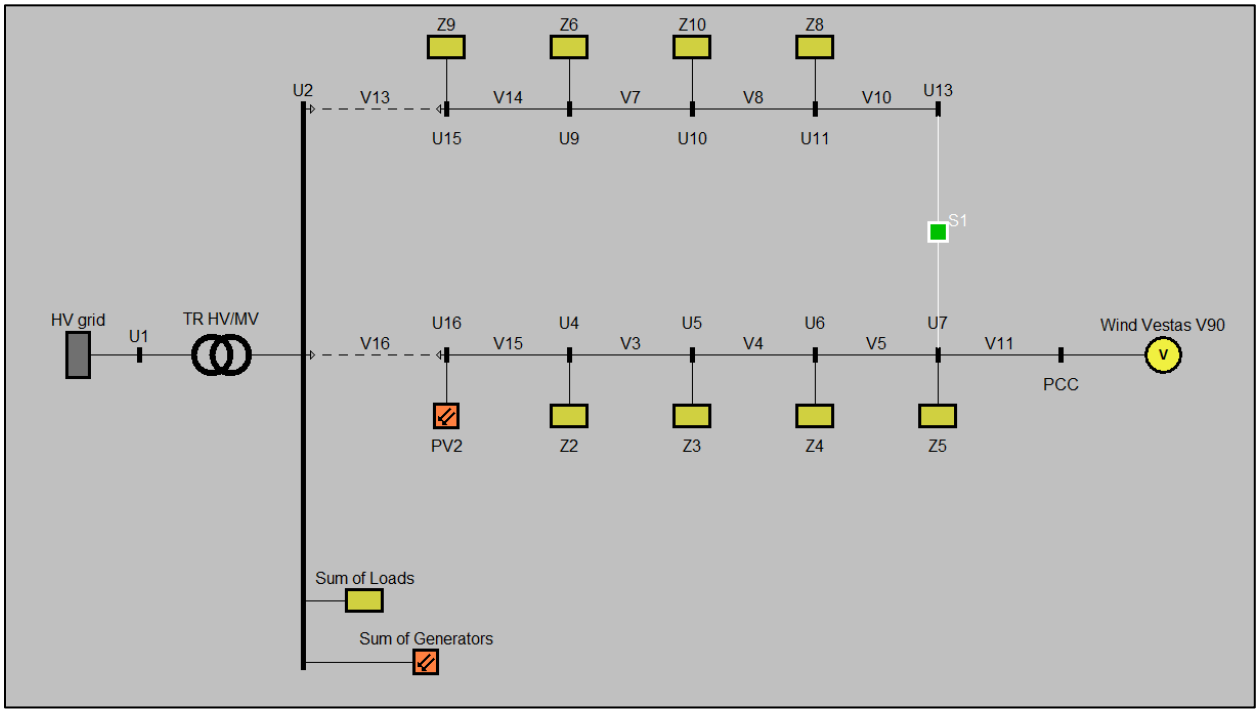

Figure 6.9 – Network scheme in case of connection of WPP and Switch S1 is opened

In this case, we will find Load-flow calculation and voltage difference before and after the connectivity of the WPP while the Switch S1 is open. Evaluation will be made with Wind power plant Vesta V90 and PV2. Effect of the rest of the sources will be neglected (for the study purposes). When evaluating the results, we will take into consideration that the voltage difference at all nodes does not exceed the standards, which means that the node voltage after conncetivity of the WPP should not differ from the node voltage before conncetivity of the WPP by **2%** and voltages must be inside interval **±10%**. The following tables will illustrate the dU margin, the voltage levels at each node, and the current distribution in branches (Overhead power lines).

- **dU margin**

	dUa before[%]	dUa after[%]	Δ dUa	dUb before[%]	dUb after[%]	Δ dUb	dUc before[%]	dUc after[%]	Δ dUc
U2	-3,488	-3,625	0,137	-3,488	-3,625	0,137	-3,488	-3,625	0,137
U1	-4,153	-4,21	0,057	-4,153	-4,21	0,057	-4,153	-4,21	0,057
U15	-3,459	-3,596	0,137	-3,459	-3,596	0,137	-3,459	-3,596	0,137
U9	-3,395	-3,532	0,137	-3,395	-3,532	0,137	-3,395	-3,532	0,137
U10	-3,214	-3,352	0,138	-3,214	-3,352	0,138	-3,214	-3,352	0,138
U11	-3,169	-3,306	0,138	-3,169	-3,306	0,138	-3,169	-3,306	0,138
U13	-3,169	-3,307	0,138	-3,169	-3,307	0,138	-3,169	-3,307	0,138
U16	-3,448	-3,648	0,2	-3,448	-3,648	0,2	-3,448	-3,648	0,2
U4	-2,759	-3,817	1,058	-2,759	-3,817	1,058	-2,759	-3,817	1,058
U5	-2,226	-4,143	1,917	-2,226	-4,143	1,917	-2,226	-4,143	1,917
U6	-2,039	-4,3	**2,261**	-2,039	-4,3	**2,261**	-2,039	-4,3	**2,261**
U7	-1,935	-4,441	**2,506**	-1,935	-4,441	**2,506**	-1,935	-4,441	**2,506**
PCC	-1,935	-4,595	**2,66**	-1,935	-4,595	**2,66**	-1,935	-4,595	**2,66**

- **Condition at nodes**

	Ua [kV]	αa [deg]	Ub [kV]	αb [deg]	Uc [kV]	αc [deg]	dUna [%]	dUnb [%]	dUnc [%]	Zk [Ω]	α [deg]	Sk [MVA]
U2	22,798	29,102	22,798	-90,898	22,798	149,102	-3,625	-3,625	-3,625	2,938	85,913	164,738
U1	114,631	29,828	114,631	-90,172	114,631	149,828	-4,21	-4,21	-4,21	15,125	81,467	799,997
U15	22,791	29,092	22,791	-90,908	22,791	149,092	-3,596	-3,596	-3,596	3,466	78,652	139,656
U9	22,777	29,057	22,777	-90,943	22,777	149,057	-3,532	-3,532	-3,532	7,062	66,275	68,534
U10	22,737	29,015	22,737	-90,985	22,737	149,015	-3,352	-3,352	-3,352	18,5	44,923	26,161
U11	22,727	29,004	22,727	-90,996	22,727	149,004	-3,306	-3,306	-3,306	24,495	41,915	19,759
U13	22,728	29,004	22,728	-90,996	22,728	149,004	-3,307	-3,307	-3,307	31,544	38,424	15,343
U16	22,803	29,125	22,803	-90,875	22,803	149,125	-3,648	-3,648	-3,648	3,195	81,985	151,468
U4	22,84	29,413	22,84	-90,587	22,84	149,413	-3,817	-3,817	-3,817	7,53	57,571	64,273
U5	22,911	29,747	22,911	-90,253	22,911	149,747	-4,143	-4,143	-4,143	12,222	51,367	39,599
U6	22,946	29,888	22,946	-90,112	22,946	149,888	-4,3	-4,3	-4,3	14,121	50,047	34,276
U7	22,977	29,971	22,977	-90,029	22,977	149,971	-4,441	-4,441	-4,441	15,289	48,69	31,657
PCC	23,011	30,013	23,011	-89,987	23,011	150,013	-4,595	-4,595	-4,595	15,963	47,71	**30,32**

- **Condition at branches**

	Node	Ia [A]	αa [deg]	Ib [A]	αb [deg]	Ic [A]	αc [deg]	P [kW]	Q [kVAr]	S [kVA]
Sum of Loads	U2	177,276	-14,968	177,276	-134,968	177,276	105,032	6790	1701,73	6999,999
HV grid	U1	19,256	141,445	19,256	21,445	19,256	-98,555	-2996,85	-2373,87	3823,131
TR HV/MV	U1	19,256	-38,555	19,256	-158,555	19,256	81,445	2996,847	2373,865	3823,131
	U2	94,009	142,159	94,009	22,159	94,009	-97,841	-2966,84	-2231,02	3712,084
V13	U2	12,728	-8,245	12,728	-128,245	12,728	111,755	498,466	64,271	502,592
	U15	12,892	167,4	12,892	47,4	12,892	-72,6	-498,342	-103,132	508,901
V14	U15	5,094	-10,391	5,094	-130,391	5,094	109,609	198,342	33,13	201,09
	U9	5,111	168,547	5,111	48,547	5,111	-71,453	-198,241	-36,776	201,623
V7	U9	3,389	-9,448	3,389	-129,448	3,389	110,552	132,241	19,776	133,711
	U10	3,421	167,489	3,421	47,489	3,421	-72,511	-132,027	-26,925	134,744
V8	U10	1,695	-9,533	1,695	-129,533	1,695	110,467	66,027	9,924	66,768
	U11	1,712	167,409	1,712	47,409	1,712	-72,591	-66	-13,542	67,375
V10	U11	0,088	89,004	0,088	-30,996	0,088	-150,996	0	-3,458	3,458
	U13	0	90	0	-90	0	90	0	0	0
V16	U2	35,482	-161,514	35,482	78,486	35,482	-41,514	-1321,63	465,017	1401,051
	U16	35,649	19,235	35,649	-100,765	35,649	139,235	1322,109	-484,096	1407,949
V15	U16	24,156	-150,384	24,156	89,616	24,156	-30,384	-822,109	484,096	954,05
	U4	24,204	29,809	24,204	-90,191	24,204	149,809	825,889	-484,463	957,495
V3	U4	30,328	-160,377	30,328	79,623	30,328	-40,377	-1125,89	414,462	1199,751
	U5	30,36	19,79	30,36	-100,21	30,36	139,79	1131,841	-412,916	1204,809
V4	U5	33,109	-163,309	33,109	76,691	33,109	-43,309	-1256,84	382,918	1313,878
	U6	33,12	16,754	33,12	-103,246	33,12	136,754	1259,677	-381,902	1316,296
V5	U6	35,948	-165,852	35,948	74,148	35,948	-45,852	-1384,68	351,904	1428,694
	U7	35,952	14,176	35,952	-105,824	35,952	134,176	1387,061	-351,11	1430,81
V11	U7	50,181	-179,997	50,181	60,003	50,181	-59,997	-1997,06	1,115	1997,062
	PCC	50,181	0,013	50,181	-119,987	50,181	120,013	2000	0	2000
Z9	U15	7,804	-14,042	7,804	-134,042	7,804	105,958	300	70,002	308,059
Wind Vestas V90	PCC	50,181	-179,987	50,181	60,013	50,181	-59,987	-2000	0	2000
PV2	U16	12,66	179,125	12,66	59,125	12,66	-60,875	-500	0	500
S1	U13	0	0	0	0	0	0	0	0	0
	U7	0	0	0	0	0	0	0	0	0
Sum of Generators	U2	75,975	179,102	75,975	59,102	75,975	-60,898	-3000	0	3000
Z6	U9	1,728	-15,387	1,728	-135,387	1,728	104,613	66	17	68,154
Z10	U10	1,731	-15,429	1,731	-135,429	1,731	104,571	66	17,001	68,154
Z8	U11	1,731	-15,44	1,731	-135,44	1,731	104,56	66	17	68,154
Z2	U4	7,787	-13,721	7,787	-133,721	7,787	106,279	300	70,002	308,059
Z3	U5	3,239	-13,748	3,239	-133,748	3,239	106,252	125	29,999	128,549
Z4	U6	3,234	-13,607	3,234	-133,607	3,234	106,393	125	29,999	128,549
Z5	U7	17,671	-29,874	17,671	-149,874	17,671	90,126	610	349,995	703,276

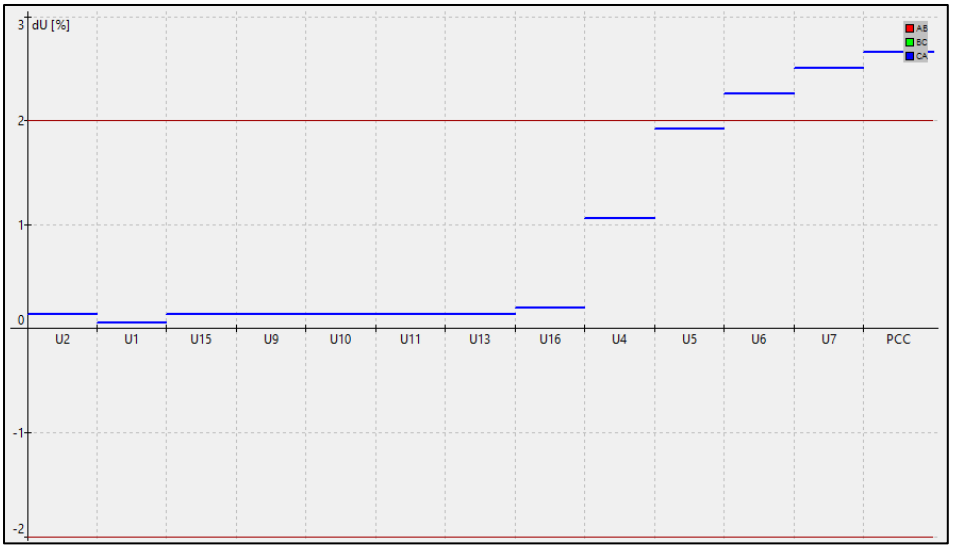

Figure 6.10 – ΔdU[%] after and before connectivity of WPP with Switch S1 opened

In this case, ΔdU is over the limit at nodes U6 **(2,261%)**, U7 **(2,506%)**, and PCC **(2,66%)**. One way for voltage change elimination is grid reconfiguration. Besides, short circuit power at node PCC was recorded at **Sk = 30.32 MVA.**

3) 2MW WIND POWER IS CONNECTED, SWITCH S1 IS CLOSED

In this case, the same calculations will be done as in case 2) but while switch S1 is closed. And we will be comparing both results and evaluate which conncetion is more suitable for meeting the standards.

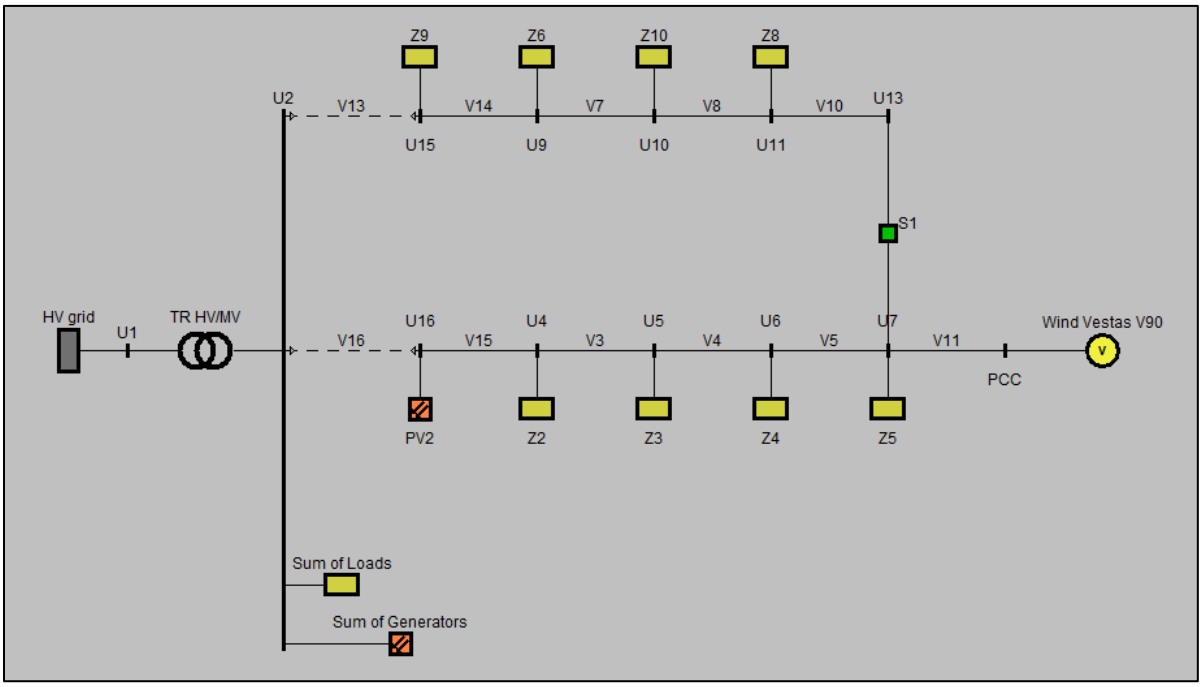

Figure 6.11 – Network scheme in case of connection of WPP and Switch S1 is closed

- **dU margin**

	dUa before[%]	dUa after[%]	Δ dUa	dUb before[%]	dUb after[%]	Δ dUb	dUc before[%]	dUc after[%]	Δ dUc
U2	-3,489	-3,629	0,14	-3,489	-3,629	0,14	-3,489	-3,629	0,14
U1	-4,154	-4,211	0,057	-4,154	-4,211	0,057	-4,154	-4,211	0,057
U15	-3,445	-3,613	0,169	-3,445	-3,613	0,169	-3,445	-3,613	0,169
U9	-3,286	-3,595	0,309	-3,286	-3,595	0,309	-3,286	-3,595	0,309
U10	-2,747	-3,771	1,023	-2,747	-3,771	1,023	-2,747	-3,771	1,023
U11	-2,523	-3,904	1,381	-2,523	-3,904	1,381	-2,523	-3,904	1,381
U13	-2,309	-4,148	1,838	-2,309	-4,148	1,838	-2,309	-4,148	1,838
U16	-3,457	-3,646	0,188	-3,457	-3,646	0,188	-3,457	-3,646	0,188
U4	-2,906	-3,709	0,803	-2,906	-3,709	0,803	-2,906	-3,709	0,803
U5	-2,51	-3,928	1,418	-2,51	-3,928	1,418	-2,51	-3,928	1,418
U6	-2,377	-4,042	1,664	-2,377	-4,042	1,664	-2,377	-4,042	1,664
U7	-2,309	-4,148	1,838	-2,309	-4,148	1,838	-2,309	-4,148	1,838
PCC	-2,309	-4,302	**1,992**	-2,309	-4,302	**1,992**	-2,309	-4,302	**1,992**

- **Condition at nodes**

	Ua [kV]	αa [deg]	Ub [kV]	αb [deg]	Uc [kV]	αc [deg]	dUna [%]	dUnb [%]	dUnc [%]	Zk [Ω]	α [deg]	Sk [MVA]
U2	22,798	29,104	22,798	-90,896	22,798	149,104	-3,629	-3,629	-3,629	2,938	85,913	164,738
U1	114,632	29,829	114,632	-90,171	114,632	149,829	-4,211	-4,211	-4,211	15,125	81,467	799,997
U15	22,795	29,107	22,795	-90,893	22,795	149,107	-3,613	-3,613	-3,613	3,456	78,726	140,042
U9	22,791	29,171	22,791	-90,829	22,791	149,171	-3,595	-3,595	-3,595	6,608	65,995	73,249
U10	22,83	29,397	22,83	-90,603	22,83	149,397	-3,771	-3,771	-3,771	12,231	47,422	39,573
U11	22,859	29,52	22,859	-90,48	22,859	149,52	-3,904	-3,904	-3,904	12,731	46,355	38,016
U13	22,912	29,664	22,912	-90,336	22,912	149,664	-4,148	-4,148	-4,148	11,292	49,826	42,861
U16	22,802	29,12	22,802	-90,88	22,802	149,12	-3,646	-3,646	-3,646	3,193	82,007	151,577
U4	22,816	29,292	22,816	-90,708	22,816	149,292	-3,709	-3,709	-3,709	6,922	58,478	69,918
U5	22,864	29,511	22,864	-90,489	22,864	149,511	-3,928	-3,928	-3,928	9,913	52,346	48,827
U6	22,889	29,607	22,889	-90,393	22,889	149,607	-4,042	-4,042	-4,042	10,826	50,931	44,708
U7	22,912	29,664	22,912	-90,336	22,912	149,664	-4,148	-4,148	-4,148	11,292	49,826	42,861
PCC	22,946	29,706	22,946	-90,294	22,946	149,706	-4,302	-4,302	-4,302	11,962	48,455	**40,463**

- **Condition at nodes**

	Node	Ia [A]	αa [deg]	Ib [A]	αb [deg]	Ic [A]	αc [deg]	P [kW]	Q [kVAr]	S [kVA]
Sum of Loads	U2	177,269	-14,966	177,269	-134,966	177,269	105,034	6790	1701,73	6999,999
HV grid	U1	19,213	141,463	19,213	21,463	19,213	-98,537	-2990,94	-2367,68	3814,656
TR HV/MV	U1	19,213	-38,537	19,213	-158,537	19,213	81,463	2990,935	2367,68	3814,656
	U2	93,796	142,179	93,796	22,179	93,796	-97,821	-2960,94	-2225,11	3703,819
V13	U2	6,078	-62,668	6,078	177,332	6,078	57,332	113,521	211,465	240,009
	U15	6,963	113,488	6,963	-6,512	6,963	-126,512	-113,488	-250,414	274,93
V14	U15	6,572	-136,845	6,572	103,155	6,572	-16,845	-186,512	180,412	259,49
	U9	6,639	43,751	6,639	-76,249	6,639	163,751	186,681	-183,964	262,093
V7	U9	7,672	-147,373	7,672	92,627	7,672	-27,373	-252,681	166,963	302,86
	U10	7,776	33,767	7,776	-86,233	7,776	153,767	253,782	-173,575	307,463
V8	U10	9,005	-154,515	9,005	85,485	9,005	-34,515	-319,782	156,575	356,056
	U11	9,046	26,013	9,046	-93,987	9,046	146,013	320,533	-159,762	358,142
V10	U11	10,407	-160,209	10,407	79,791	10,407	-40,209	-386,533	142,762	412,054
	U13	10,438	20,247	10,438	-99,753	10,438	140,247	387,801	-145,634	414,245
V16	U2	25,143	-162,586	25,143	77,414	25,143	-42,586	-942,582	311,916	992,851
	U16	25,302	18,475	25,302	-101,525	25,302	138,475	942,823	-331,201	999,305
V15	U16	14,002	-144,086	14,002	95,914	14,002	-24,086	-442,823	331,201	552,98
	U4	14,058	36,221	14,058	-83,779	14,058	156,221	444,096	-333,793	555,553
V3	U4	19,977	-161,188	19,977	78,812	19,977	-41,188	-744,096	263,791	789,471
	U5	20,009	19,067	20,009	-100,933	20,009	139,067	746,68	-265,228	792,387
V4	U5	22,798	-165,387	22,798	74,613	22,798	-45,387	-871,68	235,229	902,862
	U6	22,808	14,705	22,808	-105,295	22,808	134,705	873,025	-235,532	904,239
V5	U6	25,702	-168,756	25,702	71,244	25,702	-48,756	-998,025	205,533	1018,969
	U7	25,706	11,284	25,706	-108,716	25,706	131,284	999,244	-205,486	1020,153
V11	U7	50,322	179,696	50,322	59,696	50,322	-60,304	-1997,05	1,126	1997,045
	PCC	50,322	-0,294	50,322	-120,294	50,322	119,706	2000	0	2000
Z9	U15	7,803	-14,027	7,803	-134,027	7,803	105,973	300	70,002	308,059
Wind Vestas V90	PCC	50,322	179,706	50,322	59,706	50,322	-60,294	-2000	0	2000
PV2	U16	12,66	179,12	12,66	59,12	12,66	-60,88	-500	0	500
S1	U13	10,438	-159,753	10,438	80,247	10,438	-39,753	-387,801	145,634	414,245
	U7	10,438	20,247	10,438	-99,753	10,438	140,247	387,801	-145,634	414,245
Sum of Generators	U2	75,973	179,104	75,973	59,104	75,973	-60,896	-3000	0	3000
Z6	U9	1,727	-15,273	1,727	-135,273	1,727	104,727	66	17,001	68,154
Z10	U10	1,724	-15,047	1,724	-135,047	1,724	104,953	66	17	68,154
Z8	U11	1,721	-14,924	1,721	-134,924	1,721	105,076	66	17	68,154
Z2	U4	7,795	-13,842	7,795	-133,842	7,795	106,158	300	70,002	308,059
Z3	U5	3,246	-13,984	3,246	-133,984	3,246	106,016	125	29,999	128,549
Z4	U6	3,242	-13,888	3,242	-133,888	3,242	106,112	125	29,998	128,549
Z5	U7	17,721	-30,182	17,721	-150,182	17,721	89,818	610	349,995	703,276

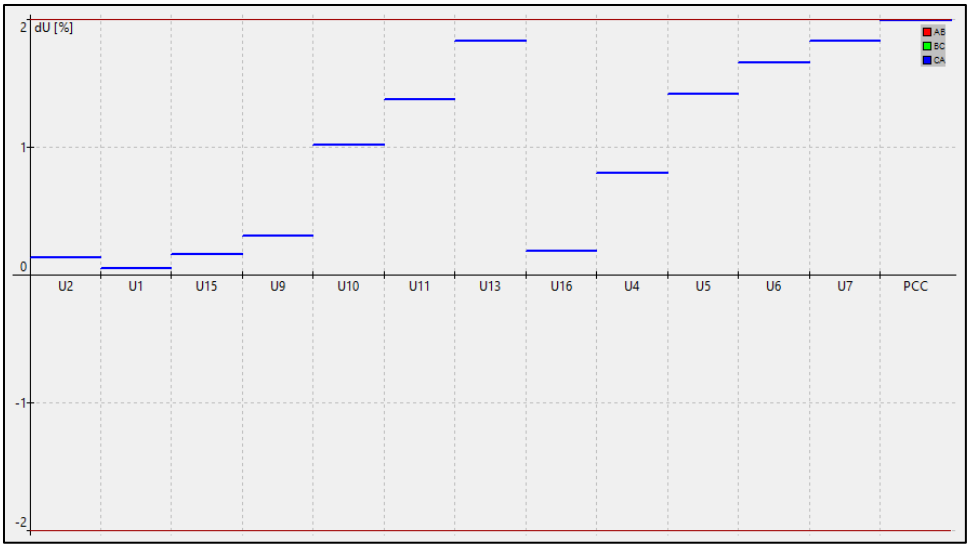

Figure 6.12 – ΔdU[%] after and before connectivity of WPP with Switch S1 closed

In this case, the maximum value of ΔdU was recorded at the node PCC **(1.992%)** which was below the maximum limit (**2%**), which mean that this configuration is valid. Also, compared to the short circuit power in case 2) **(Sk = 30.32 MVA)**, the short circuit power at the point of common coupling (PCC) has increased after switching both power lines together, **Sk = 40.463 MVA**.

Now, as we found a valid connection for the WPP to the distribution network that meets the standards, this connection will be used to evaluate the flicker effect.

- ## Short-term flicker (Pst parameter)

For the Pst parameter calculation, coefficient c is needed. Coefficient c can be found in the power source datasheet and should be used in the DNCalc software. [18]

We will select coefficient c for the worst case: When the annual average wind speed is 6 m/s, coefficient c is equal to **2.1**.

Morever, in our case, Pst in equal to Plt (in DNCalc software, Pst result is constant in time, so Pst is equal to Plt). When we evaluate the results, we will take into consideration that Plt limit is **0.46** (MV voltage level).

Node	Pst
U2	0,025
U1	0,005
U15	0,027
U9	0,051
U10	0,094
U11	0,098
U13	0,098
U16	0,028
U4	0,06
U5	0,086
U6	0,094
U7	0,098
PCC	**0,104**

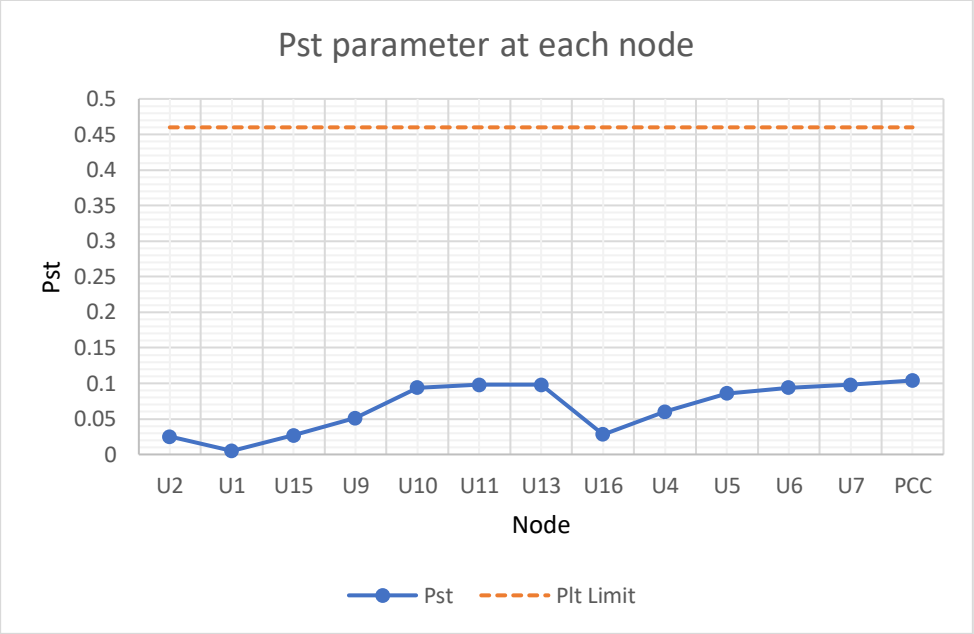

From the table and graph above, we can conclude that the Pst parameter has not exceeded the Plt limit **(0.46).** Hence, the connection is still valid after evaluating the flicker effect.

6.3.2 Analysis of calculation results

New wind power plant connectivity was evaluated from the perspective of voltage change and Flicker effect.

In the first case, where the switch S1 is opened and PCC is fed from the one side, voltage change was over the 2% limit. In the second case, where switch S1 is closed, voltage change was lower than the 2% limit.

Hence, we can conclude that:

- From the perspective of voltage change, permanent parallel operation of power lines is needed.
- From the perspective of the flicker effect, calculated Pst is lower than limit the **0.46**.

7 Conclusion

A brief explanation have been presented for the three major renewable energy sources (RES): Hydropower, Solar energy, and Wind energy. Alongside the brief explanation, the main components and the working principles of the power plants that utilize these renewable energy sources to generate power have also been explained.

The present and future usage of the RES to generate power in the European Union and Egypt was stated according to the International Renewable Energy Agency (IRENA). It was established that most countries are willing to utilize the RES to generate power to minimize the usage of other sources like Solid fuels. These plans have been constructed to cease the depletion of limited sources in energy production and to prevent the emission of harmful greenhouse gases to the environment.

A brief discussion about the impact of RES when connected to distribution network and rules for connecting RES with distribution grid has been provided.

Using the DNCalc software, a network model was designed and used to test the connectivity of a 2MW Wind power plant (Vestas V-90) at point of common coupling from the perspective of voltage change and Flicker effect. To evaluate the connectivity, different configurations of the network have been developed. The results have shown that a permanent parallel operation of power lines is needed to maintain voltage profiles that meet the standard limits. The standard limit was that the voltage difference in a distribution network must be lower than 2% of nominal voltage before and after the connection of a wind power plant. Also, we have noticed a slight increase in the short circuit power at the point of common coupling (PCC) under parallel operation of power lines Sk = 40.463 MVA compared to when the switch S1 was open Sk = 30.32 MVA. On the other hand, from the prespective of flicker effect, the calculation under the worst case showed that the Pst parameter did not exceed the limit.

8 Reference

[1] How Hydropower Works. (n.d.). Retrieved from https://www.energy.gov/eere/water/how-hydropower-works

[2] Hydropower Basics. (n.d.). Retrieved from https://www.energy.gov/eere/water/hydropower-basics

[3] Jimenez, R. (2016, October 26). How Solar Panels Work - Park City's Premier Heat Cable Installer: On Top Roofing & Electric. Retrieved from https://www.ontopsolarandelectric.com/park-city-solar-blog/2016/10/26/how-solar-panels-work

[4] Electrical4U. (2018, May 15). Working Principle of Solar Cell or Photovoltaic Cell. Retrieved from https://www.electrical4u.com/working-principle-of-photovoltaic-cell-or-solar-cell/

[5] The Inside of a Wind Turbine. (n.d.). Retrieved from https://www.energy.gov/eere/wind/inside-wind-turbine

[6] Renewable energy prospects for the European Union: Preview for Policy Makers. (n.d.). Retrieved from https://www.irena.org/publications/2018/Feb/Renewable-energy-prospects-for-the-EU

[7] WHAT ARE THE EUROPEAN GREEN DEAL AND THE ENERGY UNION ABOUT? (n.d.). Retrieved from https://ec.europa.eu/eurostat/cache/infographs/energy/bloc-1.html

[8] Renewable Energy Outlook: Egypt. (n.d.). Retrieved from https://www.irena.org/publications/2018/Oct/Renewable-Energy-Outlook-Egypt

[9] ENERGETICKÝ REGULAČNÍ ÚŘAD. *Pravidla provozování distribučních soustav*. Příloha č. 4., Praha, 2018

[10] Mwaniki, J., Lin, H., & Dai, Z. (2017). A Condensed Introduction to the Doubly Fed Induction Generator Wind Energy Conversion Systems. *Journal of Engineering*, *2017*, 1–18. doi: 10.1155/2017/2918281

[11] Edward, Clarke, Benjamin, Nicholas, Gary, Amiri, K., … McDonald. (2020, January 15). A review of wind turbine main bearings: design, operation, modelling, damage mechanisms and fault detection. Retrieved from https://www.wind-energ-sci.net/5/105/2020/

[12] DNCalc Software

[13] NORMA ČSN EN 60909-0. Zkratové proudy v trojfázových střídavých soustavách - Část 0: Výpočet proudů. 2019.

[14] DNCacl brochure, EGC - EnerGoConsult ČB s.r.o., 2017

[15] NORMA PNE 33 3430-0. *Parametry kvality elektrické energie - Část 0: Výpočetní hodnocení zpětných vlivů odběratelů a zdrojů distribučních soustav.* 2009.

[16] [number3] NORMA ČSN EN 50 160. *Charakteristiky napětí elektrické energie dodávané z veřejné distribuční sítě.* 2011.

[17] [number4] NORMA ČSN EN 60909-0. Zkratové proudy v trojfázových střídavých soustavách - Část 0: Výpočet proudů. 2019.

[18] Power Quality Measurements on the VESTAS V-902.MW VCS Short Report according to "IEC61400-21"